Technoeconomic analysis of T7 RNA polymerase manufacturing in *E.coli* for South Africa

by

Alicia Lundh

Department of Process Engineering Stellenbosch University
& Department of Chemical Engineering Lund University

December 2022

Internal supervisor: **Joaquín Gomis Fons**
External supervisor: **Professor Siew L. Tai**
Examiner: **Professor Bernt Nilsson**

Picture on front page: Vaccine syringe on map of Africa. By author using DALL.E AI Image Generator

Postal address
P.O. Box 124
SE-221 00 Lund, Sweden
Web address
www.chemeng.lth.se

Visiting address
Getingevägen 60

Telephone
+46 46-222 82 85
+46 46-222 00 00
Telefax
+46 46-222 45 26

Acknowledgement

This master thesis was conducted at Stellenbosch University, South Africa, in collaboration with the Department of Chemical Engineering at Lund University. This project resulted from a search for opportunities to pursue my dream of conducting a master thesis related to global health. My passion for global health sparked five years ago just before starting my degree, when I saw the deathly outcomes from lack of access to pharmaceuticals and medical devices in Zimbabwe. I am happy and proud to end my Chemical Engineering degree in Pharmaceutical Science by coming back to a neighboring country and to conduct a master thesis related to vaccine access on the African continent.

First and foremost, I would like to thank my external supervisor Professor Siew L. Tai at Stellenbosch University. Thank you for giving me the opportunity to come all the way to South Africa from Sweden, and your invitation to work on a project related to global health. I cannot express enough gratitude for this, as well as for your guidance in the project and your genuine kindness and efforts for me to have a great experience during my stay in South Africa.

I would also like to express my sincere gratitude to my internal supervisor Postdoctoral research fellow Joaquín Gomis Fons from Lund University. I truly appreciate your generous assistance throughout the project. Thank you, Joaquín Gomis Fons and my examiner Professor Bernt Nilsson, for agreeing to this collaboration and enabling me to go to Stellenbosch.

Special thanks to my research group at Stellenbosch University, Reitumetse Kholumo and Moleboheng Ntsetselane, for your support and giving me a warm welcome to South Africa. Thank you also to everyone at Stellenbosch University who helped with the project and for your hospitality, with which it was easy for me to see South Africa as my second home.

Finally, I would like to thank my friends and family. Your never-ending support, throughout my search for a master thesis in Africa, heavy visa application and other practicalities, as well as being there to bounce ideas off, is much appreciated.

Alicia Lundh
Stellenbosch, December 2022

Abstract

The enzyme, T7 RNA polymerase (T7 RNAP), is one of the most expensive raw materials required for mRNA vaccine production. As part of establishing South African manufacturing of mRNA vaccine, it is of interest to investigate the feasibility and profitability of South African manufacturing of T7 RNAP.

This project scaled up present lab-scale knowledge on T7 RNAP production and used SuperPro designer as a tool to model a T7 RNAP process. In order to achieve South African annual demand of the enzyme required in mRNA vaccine manufacturing, the model suggested a main bioreactor size of 15L and operating approximately 1.5 months a year. The economic assessment for the base case model, concluded the NPV to be $19,250,000, IRR to be 21.33% with a 3.92 years payback time. The results also imply that it is more affordable to manufacture T7 RNA polymerase in South Africa than purchase the enzyme from an international supplier.

The sensitivity analysis showed that the model was sensitive to changes in revenue. If T7 RNAP can be sold for approximately $2 million per gram, instead of $136 000 as the base case, higher profitability such as IRR of 148% and 0.23 years payback time can be expected. The model was also sensitive to changes in process parameters of both biomass yield and T7 RNAP yield. The evaluation of result validity suggests more research needs to be performed to obtain accurate and modern yields for industrial scale.

Overall, the results indicate that South African T7 RNAP production is profitable and has capacity for more production annually than demanded in South Africa. Thus, it is recommended to investigate the possibilities to manufacture other required enzymes for mRNA vaccine production with the same process, to enable an independent value chain for South Africa.

Popular Science abstract

The COVID pandemic revealed the African continent´s vulnerability in access to vaccines, when the COVID vaccine reached African countries later than other regions. In order to solve this problem WHO decided in 2021 to support African manufacturing by funding an mRNA vaccine technology transfer hub in South Africa. Ensuring sustainable mRNA vaccine manufacturing in South Africa, local access and profitable production of raw materials required for the vaccine are essential. The enzyme T7 RNA polymerase is one of the most expensive raw materials required for mRNA vaccine production. This is why it is of interest to investigate feasibility and profitability of South African manufacturing of T7 RNA polymerase.

Currently, the T7 RNA polymerase process can be found in open literature for lab-scale but not pilot or industrial scale. Neither can any indication of profitability for T7 RNA polymerase manufacturing be found. This study aimed to fill that gap by upscaling present lab-scale knowledge on T7 RNA polymerase production and model the process to investigate its economic feasibility in South Africa.

This project modelled the T7 RNA polymerase process using a simulation software. The results indicated that South African T7 RNA polymerase production is profitable and feasible. It was also shown that it is more affordable to manufacture T7 RNA polymerase in South Africa than purchase the enzyme from an international supplier.

In summary, this thesis work contributes to the understanding of how to produce an enzyme required for mRNA vaccine production and proved it is profitable for this raw material to be produced in South Africa. The results open for new research opportunities to enable an entire independent value chain for South African mRNA vaccine. This would contribute to establish vaccine access for the African continent, so to be well equipped for next pandemic as well as meeting current needs of other diseases.

Table of contents

1 Introduction

1.1 Problem statement

Recent success of the mRNA vaccines developed for COVID has contributed to a greater interest in mRNA vaccines. COVID outbreak emphasized the need for a flexible and efficient vaccine production, which mRNA vaccine production can provide [1]. The concept of using exogenous mRNA to produce proteins *in vivo* is relatively new. Mice tests were first reported in 1990, but not until 2020 Moderna´s and Pfizer/BioNtech´s vaccines against COVID were the first mRNA vaccines approved by the FDA [2]. However, the vaccines did not reach everyone. According to the World Health Organization (WHO) Africa [3], Africa received COVID vaccines later than other regions in the world and in limited quantities. Thus, in order to better control outbreaks in the future as well as improving immunization of childhood diseases, more extensive African manufacturing of vaccines is needed [3]. WHO announced on 21st, of June 2021 that the Medicines Patent Pool and the Act-Accelerator/COVAX will support South African consortium to establish first mRNA vaccine technology transfer hub. The hub consists of Afrigen Biologics and Vaccines which establishes the technology, South African Medical Research Council (SAMRC) which provides the research and Biovac who will be the first manufacturer. In July 2021, the hub was ready to operate at Afrigen, located in Cape Town [4].

The principle of mRNA vaccine, is to introduce mRNA that codes for a pathogenic protein into human cells [2]. The cell will synthesize the pathogenic protein which will generate an immune response that leads to protection from the actual pathogen [2]. One vital step of the mRNA vaccine manufacturing, is the In Vitro Transcription (IVT) where the mRNA is produced [2]. In that step, a RNA polymerase enzyme called T7 (T7 RNAP), is used to catalyse the synthesis of the mRNA from a DNA template, see Figure 1 [1].

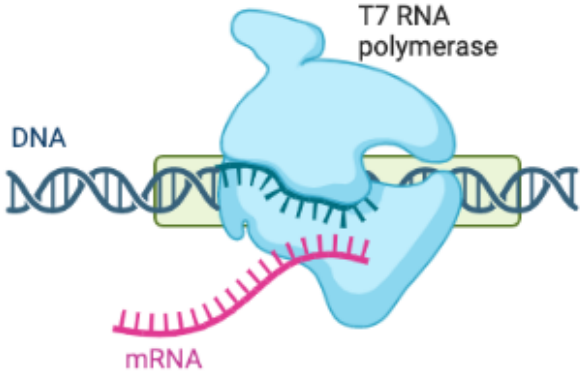

Figure 1 DNA transcribed into mRNA by T7 RNAP. Figure adjusted from [1]. Figure created by using BioRender.com.

Based on a model of mRNA vaccine process, presented in an article by Ferreira and Petrides, raw materials are responsible for 97% of the annual production costs [2]. T7 RNAP stands alone for 34% of the raw material costs, and thereby is the most expensive raw material reported in the article by Ferreira and Petrides [2]. Thus, it is believed there is potential for

most cost impact on the mRNA vaccine manufacturing by optimizing the production of T7 RNAP. Moreover, according to a report by Public Citizen on how to make enough vaccine for the world in one year, the sudden increase of T7 RNAP demand can lead to that suppliers might be struggling to produce enough [5].

In addition to mRNA vaccine, T7 RNAP has been widely applied in engineering genetic circuits [6]. T7 RNAP has great specificity for its promotors which can be used to produce a desired product by introducing a plasmid into *E.coli* with the gene of interest under the control of a T7 promotor [7]. T7 RNAP has been used to overexpress proteins *in vivo* and synthesize RNAs *in vitro* [7]. The large amounts of specific RNA that purified T7 RNAP can produce, are useful for any purpose requiring a specific RNA such as substrates for analysing processing reactions or RNA splicing [8].

For T7 RNAP lab applications, several lab protocols of T7 RNAP preparation can be found in literature [8]–[17]. However, no information is available on T7 RNAP process on pilot or industrial scale, even though there is commercially available T7 RNAP. Currently, to the best of the authors´ knowledge, there is no T7 RNAP manufacturing with current Good Manufacturing Practice (cGMP) certification in South Africa that can supply the upcoming vaccine production in the country. Hence, establishing manufacturing of T7 RNAP in South Africa could also contribute to South African self-determination. A vital step for South African manufacturing of T7 RNAP, is to gain understanding of its feasibility and profitability with investment and production cost of such site locally.

In addition, to the best of the authors´ knowledge, no technoeconomic analysis of T7 RNAP manufacturing in South Africa is present in open literature. This study aims to fill that gap by upscaling present knowledge on T7 RNAP synthesis, modelling the process to conduct a technoeconomic analysis.

1.2 Aim and Project Scope

The ultimate goal is a sustainable local South African manufacturing of T7 RNA polymerase. The research presented in this report aims to create a process model of T7 RNA polymerase manufacturing in South African setting and investigate its economic feasibility. The project´s hypothesis is that T7 RNAP would be more affordable to produce in South Africa than purchasing it externally.

Objectives:

- Set up process model of T7 RNAP in SuperPro Designer based on lab protocol
- Scale up model to industrial size
- Analyse economic data & modify model
- Analyse sensitivity of the model

Scope:

- In-silico simulation
- Creating model using SuperPro Designer
- T7 RNA polymerase manufacturing by using *E.coli*
- Factors scale up from lab protocol on raw materials and equipment sizing when applicable
- T7 RNAP demand based on mRNA vaccine production
- Cost estimations based on South African setting when achievable
- Process limits: starting from seed bioreactor, ending with product stream excluding cold storage, cleaning-in-place as well as sterilization-in-place
- Out of scope: T7 RNA polymerase incorporated into mRNA vaccine production

The key questions that this research aims to answer are:

- Would South African T7 RNAP production be profitable?
- How many operating hours are required to fulfil South African demand of T7 RNAP?
- What economic parameters are most sensitive in the model?
- What process parameters has largest effect on profitability?

2 Background

2.1 mRNA vaccine production

There are different process step combinations that are possible when producing mRNA vaccine [1]. One way to synthesize mRNA vaccine is with the process steps: RNA synthesis, purification and lastly nanoencapsulation, see **Error! Reference source not found.** [2]. The RNA synthesis starts with plasmid DNA (pDNA) linearization using a restriction enzyme to cut the circular DNA [2]. It is followed by In Vitro Transcription (IVT) where the mRNA is synthesized enzymatically [2]. The IVT can include the following enzymes: T7 RNAP (to catalyse the mRNA synthesis), murine ribonuclease inhibitor (to prevent degradation of the RNA formed) and pyrophosphate (to break down pyrophosphate into phosphate ions) [2]. After IVT a second enzymatic reaction takes place using the vaccinia capping enzyme and a methyl donor substrate such as 2′-O-methyltransferase enzyme [1], [18]. The vaccinia capping enzyme, is a complex consisting of two subunits (D1 and D12), where three enzymatic activities are combined in D1 (RNA triphosphatase, guanylyltransferase and guanine methyltransferase), while D12 stabilizes the D1 protein [18], [19]. Lastly in the RNA synthesis process, DNase can be added to degrade the DNA template [20].

Thereafter the purification takes place, which can involve crossflow filtration, oligo-dT chromatography, hydrophobic interaction chromatography, followed by another crossflow filtration [2]. Nanoencapsulation is the final step, where the purified mRNA is mixed with lipids to form lipid nanoparticles with mRNA strands in the middle [2]. The solvent in the solution is also replaced to a suitable formulation buffer [2].

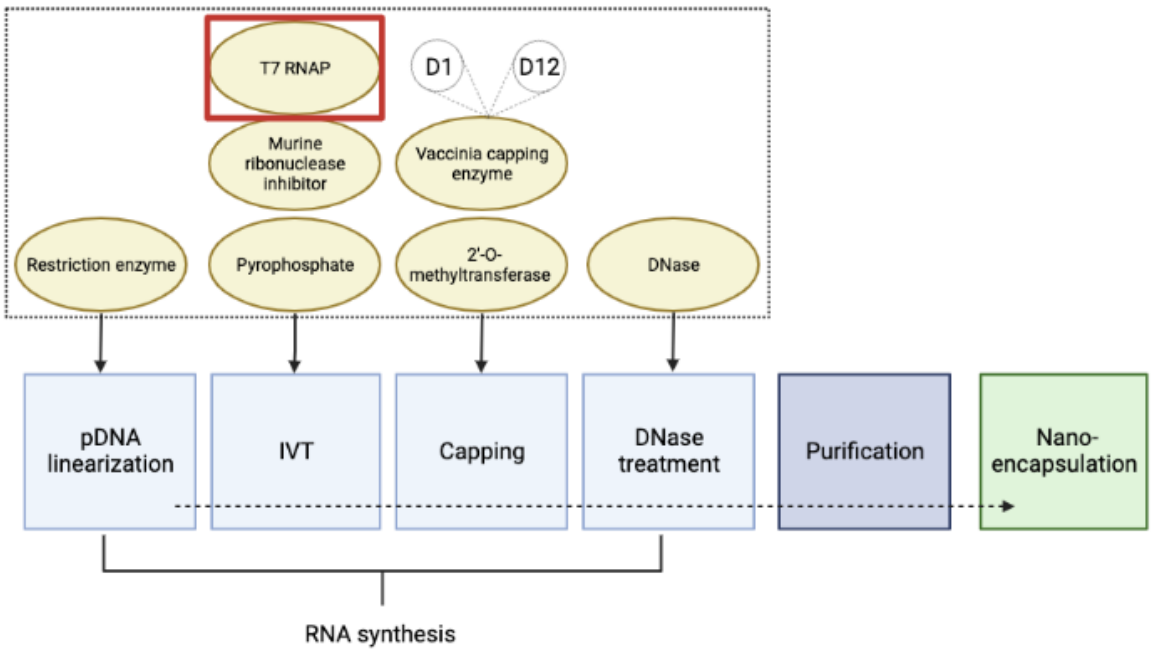

Figure 2: Schematic representation of mRNA vaccine production, adjusted from [1], [2], [18]–[20]. The three process steps are colour coded: RNA synthesis (blue), purification (purple) and nanoencapsulation (green). The figure also illustrates which enzymes are required for the different steps in the RNA synthesis. T7 RNAP is emphasized in red. Figure is created with BioRender.com.

Depending on the manufacturer, the amount of mRNA in a vaccine dose varies. Moderna´s COVID mRNA vaccine contains 100µg mRNA per vaccine dose, whereas BioNTech-Pfizer and CureVac contains 30µg and 12µg mRNA per vaccine dose respectively [5]. Consequently, more raw materials such as T7 RNAP is required for manufacturers with higher amount of mRNA. Moderna´s vaccine requires, 0.67µg (300 U[1]) T7 RNAP per vaccine dose [5]. The amount of T7 RNAP required for vaccine doses from BioNTech-Pfizer and CureVac, is 0.30µg (90 U) and 0.08µg (36 U) respectively [5]. However, in 2022 FDA approved Moderna to reduce the mRNA amount to 50µg for COVID booster dose [21].

2.2 T7 RNAP synthesis

T7 RNA polymerase is part of the enzyme family who synthesize nucleic acids (the polymerases), and originates from the bacteriophage T7 [7]. T7 RNAP can be produced upon infection of an *Escherichia coli* cell and has a transcription rate 8 times higher than the native *E.coli* RNAP [7], [22]. The early region of T7´s genome, that are induced into the *E.coli*, is transcribed by the native *E.coli* RNAP leading to the synthesis of T7 RNAP, see Figure 3 [23]. T7 RNAP is highly selective of its own promotors, directing transcription to its own DNA rather than *E.coli´*s DNA [24]. Once T7 RNAP has been produced, other products from T7 gene inactivates the native E. coli RNAP [8], making it possible for more production of T7 RNAP. However, the enzyme is only synthesized for a few minutes during infection of the host, as a result the yield of purified T7 RNAP from infected cells is not particularly good [8]. An alternative to infected cells, is to use a clone of the T7 RNAP active gene in a plasmid [8].

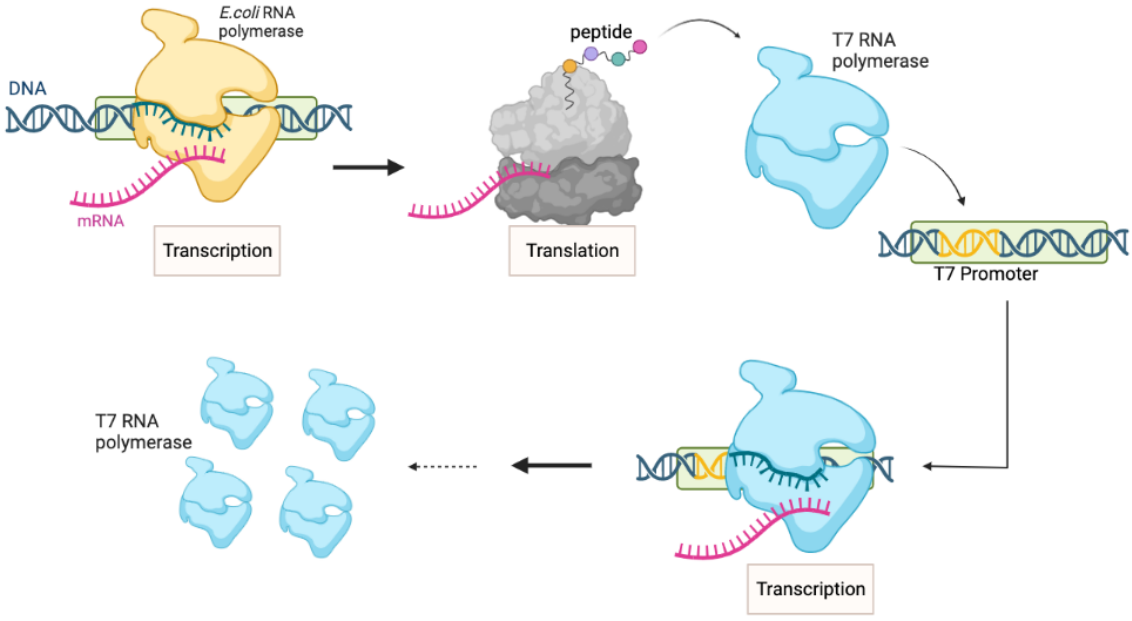

Figure 3 Synthesis of T7 RNAP in E.coli, by producing the first T7 RNAP from T7 genome using E.coli RNAP. Then, T7 RNAP selectiveness of its own promoters leads to more production of T7 RNAP. Synthesis adapted from [7], [8], [22]–[24]. Figure created by using BioRender.com.

2.3 T7 RNAP production process

A schematic representation of T7 RNAP preparation can be seen in Figure 4.

[1] Amount of T7 RNAP required in Units (U), was calculated using specific enzyme activity 450 000 U/mg T7 RNA polymerase that was found in literature [13].

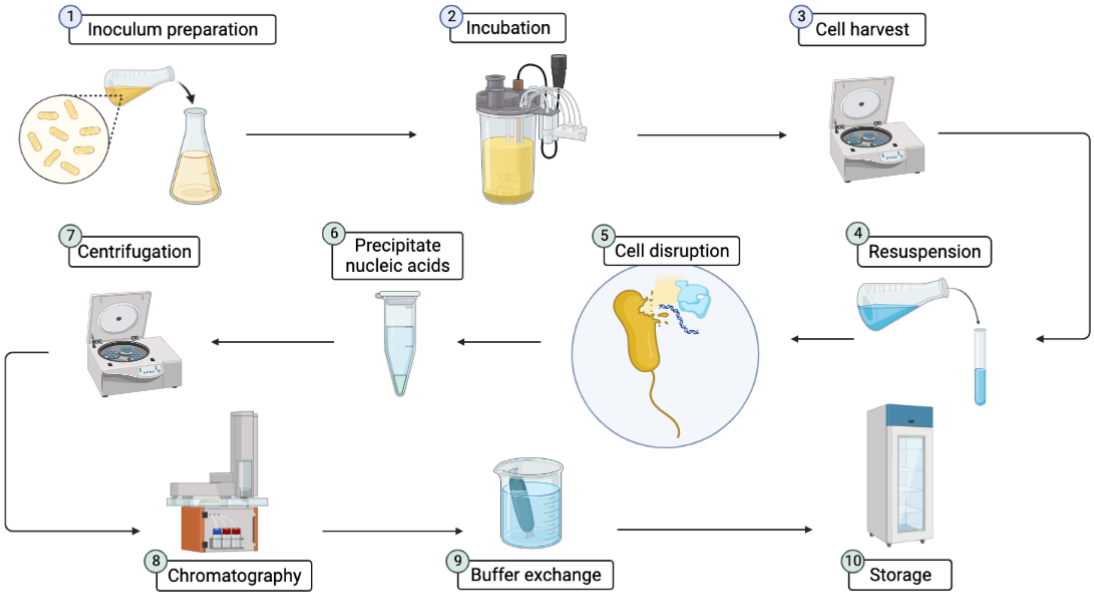

Figure 4 Schematic representation of T7 RNAP preparation lab protocol, adapted from literature [9]. Number 1-3 represent the upstream process, while number 4-10 the downstream process where the purification occurs. Figure created by using BioRender.com.

The preparation of T7 RNAP can be divided into upstream process, where the production of T7 RNAP occurs, followed by downstream process including recovery and purification of the product. The upstream process starts with preparation of inoculum, where a pre-culture is needed to start the cell growth. The *E.coli* B strain BL21 (DE3) is the most widely used host for protein production [22]. For T7 RNAP production, BL21 has been used with the plasmid pAR1219, carrying genes for T7 RNAP [13]. To address the problem of plasmid instability, antibiotics have been added 13], [25].

The pre-culture is inoculated in a growth media, for instance lysogeny broth (LB) medium [9]. Next step in T7 RNAP preparation is incubation, as seen in Figure 4, where Isopropyl β-D-1-thiogalactopyranoside (IPTG) is added. IPTG is a chemical reagent that can remove a repressor from the genome, which enables T7 RNAP binding to T7 promoter [26]. As a result, the transcription can start and allows T7 RNAP to accumulate in the cells [17].

After incubation, the cells are harvested using centrifugation, which is followed by the first step of the downstream process: resuspension, which prepares for cell disruption [9]. Since T7 RNAP is expressed intracellular, cell disruption is required to break open the cells to release their contents [27]. The organic waste left after a cell dies, the cell debris, generated from the cell disruption is separated from the product by centrifugation [27].

The next purification step in the downstream process is precipitation. Streptomycin sulphate is added to precipitate nucleic acids, which are removed with centrifugation [9]. To further separate and purify T7 RNAP from ribonucleases and other host cell proteins, ion exchange chromatography is used [13], [27]. Thereafter dialysis takes place to exchange the buffer, which will be the solution T7 RNAP is stored in [9]. Dithiothreitol (DTT) is one of the ingredients in the dialysis buffer that is added to T7 RNAP to prevent oxidative inactivation during storage [10]. The last step before storage, described in lab protocols, is to concentrate the sample where approximately 4g/L has been achieved [9], [14], [16].

3 Method

3.1 Modelling, simulation and economic assessment software

It is well known that process simulation shortens the time required for process development and allow comparison of process alternatives [28]. SuperPro Designer v12.03 (SPD) has been used to model T7 RNAP process with respect to technical and economic parameters. The software was also used to conduct an economic assessment, see 3.3 for specifics on costing.

3.2 Design basis

Since there is no available published T7 RNAP industrial process, lab protocol by Rues *et al* was applied to model a batch process, with scale up factor 10 [9]. For appropriate scale-up and input to model, other information sources on industrial enzyme production have also been used, which are presented in the following section.

3.2.1 Upstream

3.2.1.1 Microorganism

The *E.coli* strain BL21 carrying the plasmid pAR1219 was used as expression system. Several lab protocols have used an ampicillin resistance plasmid, and added ampicillin to the growth media, while a few protocols have been found to not use antibiotics [9], [13]. Antibiotics, such as ampicillin, have been used to address the problem of plasmid instability [25]. In general, plasmid-bearing cells have reduced growth since the protein production is a burden for the cell´s metabolism, compared to plasmid-free hosts [25], [29]. In order to avoid overgrowing of plasmid-free cells, antibiotic resistant genes are used as a selectable marker, and ensures survival as well as growth of plasmid-bearing cells when antibiotics are added, [25]. This work aims to model a GMP manufacturing site, hence the antibiotic kanamycin was used since it is one of the few antibiotic resistance genes that U.S. Food and Drug Administration (FDA) has approved [25], [30].

3.2.1.2 Growth media and cultivation conditions

The lab protocol from Rues *et al* used LB medium as growth media, while Zawadzki *et al* and Davanloo *et al* used M9 TB [8], [9], [12]. In general, growth media is required to contain sources of carbon, nitrogen, salts and some growth factors [31]. For the model, *E.coli* biomass was assumed to be formed in the bioreactor, based on an empirical formula of biomass and a mass stochiometric equation used for modelling purposes in literature, see equation (1) [32].

$$\underset{\textit{Glucose}}{180.16\ C_6H_{12}O_6} + \underset{\textit{Oxygen}}{93.67\ O_2} + \underset{\textit{Ammonia}}{9.97\ NH_3} \rightarrow \underset{\textit{Biomass}}{72.06\ CH_{1.8}O_{0.5}N_{0.2}} + \underset{\textit{Carbon dioxide}}{135.27\ CO_2} + \underset{\textit{Water}}{76.47\ H_2O} \quad (1)$$

It was assumed, based on equation (1), that raw materials required for the reaction was glucose, air and ammonia. Glucose was modelled as the only limiting nutrient with conversion rates 95-100%, since other models have made similar assumption and it has been shown that glucose transport in *E.coli* is the growth-limiting step [32], [33]. Consequently, the scale up factor 10 from Rues *et al* lab protocol on growth media, was applied to glucose input stream in the model. Input of air and ammonia was added in excess, although in a scale appropriate to equation (1),

see details in 7.1 Appendix 1. For the air, a compressor and air-filter was included in the model to generate a sterile air feed (as been seen in other work [32]).

Due to the scale up factor 10 on the glucose stream, the size of the main bioreactor became 15L, with approximately 10.3L working volume. The seed bioreactor was assumed to be 10% of the main bioreactor and the size 2L was chosen for commercial availability. An appropriate volume of pre-culture from the seed bioreactor was transferred to the main bioreactor to achieve initial optical density value at wavelength 600 (OD_{600}) of 0.1 [15]. OD_{600} of 0.1 was converted to 0.024 gram dry *E.coli* per litre bioreactor, using online converter and *E.coli* dry weight [34], [35]. The mass stochiometric equation for *E.coli* growth in the seed bioreactor, is shown by equation (2), where 0.50 g/g biomass yield from glucose was assumed [32].

$$180.16\ C_6H_{12}O_6 + 69.10\ O_2 + 12.46\ NH_3 \rightarrow 90.08\ CH_{1.8}O_{0.5}N_{0.2} + 103.08\ CO_2 + 68.56\ H_2O \quad (2)$$

Equation (1) was used for growth in the main bioreactor assuming 0.40 g/g biomass yield from glucose [32]. Kanamycin was added for costing purposes to both glucose streams of seed and main bioreactor in concentration of 0.1g/L [13]. IPTG was also added to the main bioreactor due to cost and achieved a final concentration of 1mM [9]. The output stream from the main bioreactor moved to a disk-stack centrifuge, modelled to separate media from cells with exiting concentration of 120g/L biomass in solid stream. Disc-stack centrifuge was chosen as it has been shown to be commonly used in bioprocessing [27].

3.2.2 Downstream

3.2.2.1 Cell disruption and yield

As the upstream process ends, it was assumed the solid stream from the centrifugation was collected in a tank where a resuspension buffer was mixed with the biomass, to prepare for cell lysis. The addition of resuspension buffer was in correlation with scale up factor 10 from Rues et al lab protocol. Further details of media contents and main process parameters are provided in 7.1 Appendix 1 Table 7.1.1 respective Table 7.1.2.

In lab protocols for T7 RNAP preparation, the main cell lysis methods used are French press [9], high-pressure homogenization [15], or sonication and centrifugation [12] ,[13], [17]. Zawadzki *et al* used egg white lysozyme followed by sonication to reduce the viscosity of the lysate and then centrifugation [12], [17]. Davanloo *et al* performed a similar procedure [8]. For industrial scale, high-pressure homogenization has been used for cell disruption, and was therefore included in the model [27], [36]. In the homogenization process, biomass was modelled to convert into its main components. The main composition of *E.coli* can be seen in Table 3.2.1.

Table 3.2.1: E.coli composition, data from ECMDB [35].

Component	**Volume %**
Water	70
Protein	17
Nucleic acids (incl. rRNA, tRNA, DNA, mRNA)	7
ribosome	6

An adjusted cell composition was made in this work, which is provided in 7.2 Appendix 2, Table 7.2.1. The cell components were adjusted to include T7 RNAP and cell debris, which was assumed to be all ribosomes and membrane proteins (which is 1/3 of the total number of proteins in cell [35]). Results from SDS-PAGE performed by Davanloo *et al*, suggests T7 RNAP represent 10-20% or more of the total protein in *E.coli* [8]. An average of 15% were used of the total protein volume to represent T7 RNAP composition in *E.coli*, see the adjusted composition in 7.2 Appendix 2, Table 7.2.1. Mass coefficients were obtained with the adjusted cell composition, which can be used in the material balance for cell disruption in the high-pressure homogenization. However, literature research was also performed to find articles that explicitly reports T7 RNAP yield, which can be converted to mass coefficients as it is required input for the model.

Different yields for T7 RNAP expressed in *E.coli* at lab-scale have been reported, see Table 3.2.2. Milligan *et al* reports 30mg of purified T7 RNAP per litre cell culture, using the *E.coli* strain BL21 and the plasmid pAR1219 [10]. Zawadzki *et al* used the same strain and plasmid as Milligan *et al*, and describe a yield of 11.25 mg purified T7 RNAP per gram *E.coli* [12]. Davanloo *et al* reports 15mg purified T7 RNAP per gram *E.coli,* using a different *E.coli* strain HMS174 [8]. The yield achieved from the three different sources in Table 3.2.2 was assumed to be expressed in wet cell weight, while for modelling purposes dry cell weight was used. Thus, volume % were adjusted to dry cell weight which was the basis for material balances required for the homogenization process. Composition and material balances for four scenarios are provided in 7.2 Appendix 2 Table 7.2.1-Table 7.2.4, including the three yields from Table 3.2.2 and composition data adjusted from Table 3.2.1. The scenario with T7 RNAP yield and biomass yield from Zawadzki *et al* was assumed to be the base case. A sensitivity analysis was made including the other scenarios, see section 3.4.

Table 3.2.2: Yields of T7 RNAP and biomass reported in T7 RNAP preparation lab protocols from literature.

Reference	**T7 RNAP Yield** [mg purified T7 RNAP /g *E.coli*]	**Biomass yield** [g *E.coli* /L culture]	**Strain/Plasmid**
Milligan *et al* [10]	3*	10**	BL21/pAR1219
Zawadzki *et al* [12]	11.25	8	BL21/pAR1219
Davanloo *et al* [8]	15	10	HMS174/pAR1219

*Converted from 30mg/L cell culture by dividing with biomass yield.
**Refers to Davanloo *et al*

3.2.2.2 Purification

In order to purify T7 RNAP from other *E.coli* intracellular components, the cell debris was separated from the solution by disk-stack centrifugation, which was assumed to remove 100% of the debris. The nucleic acids were assumed to be fully precipitated by the addition of streptomycin sulphate and was separated with another disk-stack centrifuge with the assumption of 100% nucleic acid removal and 5% protein (excluding T7 RNAP) removal.

To further purify the solution containing T7 RNAP, a 50 mL ion exchange chromatography column was modelled. Sizing of the column volume was based on Q Sepharose binding capacity for the protein BSA of 42mg/mL resin [37], the assumptions that 70% of the column volume was resin while the rest was void as well as the binding capacity utilization was 70%. To finalize the column volume calculation, the amount of T7 RNAP loaded to the column in the model was taken into consideration. Details of the calculations can be viewed in 7.3 Appendix 3. The column was washed with equilibrium buffer (content details in 7.1 Appendix

1 Table 7.1.1), and eluted with sodium chloride. The main solution exiting the chromatograph was assumed to solely contain T7 RNAP, sodium chloride and water, while the rest were modelled to be washed out of the column.

3.2.2.3 Formulation

To adjust the buffer exchange step for industrial scale, a diafiltration unit was used, where the buffer was exchanged to a formulation buffer including DTT. Milligan *et al* claims T7 RNAP is stable for long periods of time, but suggests to add DTT every 6 months during storage [10]. More recent research adds glycerol to a final concentration of 50% as a final step and then store at -80°C [9], [16]. Schwarz *et al* propose samples can be stored at -70°C for years, and at -20°C for months [11]. In our model, glycerol was added to a final concentration of 50%, although it does not include a final storage tank with cooling, instead it is ended with a product stream. This was done to be able to model a revenue stream.

3.2.3 Annual throughput

A targeted annual throughput amount for T7 RNAP was set to 38.1g. This was based on future demands estimations of mRNA vaccine in South Africa. It was assumed that mRNA vaccine will be able to cover all kinds of vaccines required yearly for an individual in South Africa. Thus, three vaccine doses per individual were considered to cover for instance annual vaccine dose of COVID, Zika and influenza. Future demands were also based on 60 million people as South Africa´s population size and the South African population vaccination rate from two doses of COVID vaccine which is approximately 32% [38], [39]. The amount of T7 RNAP required per vaccine dose was assumed based on Moderna´s COVID vaccine, which is presented in section 2.1.

As the annual throughput was set, the annual operating time available was varied to keep the scale up factor 10 from the lab protocol on the process and thereby keeping reasonable production scale size of bioreactors.

3.2.4 Other process assumptions

Cleaning-in-place (CIP) and sterilization-in-place (SIP) systems were not included in the model as it is stated out of scope in section 1.2. However, an estimate of duration for cleaning was included as set-up time for each equipment, which also includes labour costs for cleaning. Total cleaning time for the bioreactors was estimated to 8h, while other equipment to 1h. Exceptions were made for the chromatograph where washing and regeneration already were included, as well as air compression and filtration since they were assumed to not need cleaning.

According to lab protocols in Rues *et al* and Schnieders *et al*, centrifugation for cell harvest as well as following purification steps should be performed at 4°C for enzyme stability [9], [15]. At industrial scale, electrical cooling in centrifuges is assumed. However, in SuperPro Designer electricity could not be used as cooling agent for centrifuges, high-pressure homogenization or diafiltration. Glycol was instead used in the model as cooling agent for the mentioned equipment types. The buffers, streptomycin sulphate and the solutions added to the chromatograph were assumed to be refrigerated and modelled to be added at 4°C. However, costing for refrigeration was not included in the model, since a cold room was assumed to be included in the facility. Although for the tanks where resuspension buffer and streptomycin sulphate were added, an electrical cooling step was used.

3.3 Economic Assessment

The economic assessment was performed using SuperPro Designer´s tools for economic calculation. Cost estimations were made for raw material, utilities and labour based on a South African setting. The equipment cost provided by SuperPro designer was used since the built-in correlations for most equipment are suitable for fine chemicals and pharmaceuticals [40]. To adjust the equipment costs, South African inflation rate was added as an economic evaluation parameter in SuperPro Designer. Key parameters for the economic assessment are provided in 7.4 Appendix 4 Table 7.4.1.

3.3.1 Cost estimations

The cost of raw materials can be viewed in Table 3.3.1, which were based on market price from Alibaba platform or by Ferreira *et al* [32], [41]. The costs obtained from Ferreira *et al,* were updated from 2017 to 2022 (*n* number of years) by inflation rate, *i*, with equation (3), where *P* is the cost 2017 and *F* is the cost 2022 [42]. The inflation rate was assumed to be the average world inflation from 2018 to 2022, which was 3.48% [43]. The raw material prices from Ferreira *et al* shown in Table 3.3.1 are the adjusted cost for 2022.

$$F = P(1+i)^n \tag{3}$$

In difference to the other raw materials, streptomycin sulphate cost was obtained from Sigma Aldrich, which was assumed to provide for lab scale purposes and not industrial scale [44]. The higher cost shown in Table 3.3.1 were therefore assumed to include shipping as well as taxes and custom fees. For all other raw materials, a shipping cost was added to cover transport cost to South Africa. The shipping cost was estimated to 19.01 USD/kg based on highest weight cost (R9140/27.5kg) for export from South Africa available in DHL Tariff guide [45]. Moreover, Value-Added Tax (VAT) of 15% was added as well as 10% which was assumed to cover custom fees [46].

Table 3.3.1: Cost of raw materials. Except were indicated, the prices were market prices obtained at the Alibaba platform or by Ferreira et al. For the latter an inflation rate calculated was made to adjust prices from 2017 to 2022. For the final cost, shipment cost as well as 15% VAT and 10% for customs were added.

Raw material	**Price [USD/kg]**	**Source**	**Shipping added [USD/kg]**	**Final cost (25% added) [USD/kg]**
β-mercaptoethanol	10.00	Alibaba	29.01	36.27
Ammonia gas	0.35	Ferreira *et al*	19.36	24.20
Dipotassium phosphate	1.48	Ferreira *et al*	20.49	25.62
DTT	18.00	Alibaba	37.01	46.27
EDTA Disodium	3.14	Ferreira *et al*	22.16	27.69
Glucose	0.76	Ferreira *et al*	19.77	24.71
Glycerol	0.70	Ferreira *et al*	19.71	24.64
IPTG	689.13	Ferreira *et al*	708.14	885.18
Kanamycin sulphate	36.37	Ferreira *et al*	55.39	69.23
Sodium Chloride	0.05	Alibaba	19.07	23.84
Streptomycin sulphate	839.00	Sigma	Incl.	839.00 (incl.)
Tris_HCl	50.00	Alibaba	69.01	86.27

Another material used in the process was Water for Injection (WFI), which cost data are provided in 7.4 Appendix 4 Table 7.4.1. Water purification process was excluded from the model presented, however for costing purposes a purification process was considered. In 7.4 Appendix 4 Table 7.4.1 utilities costs are also provided. The electricity cost was locally obtained for Cape Town area, based on the assumption that a T7 RNAP factory could be built in Cape Town area since it would be close to the potential demand for mRNA vaccines from the vaccine manufacturer Biovac. Loadshedding and generator costs were not included in the electricity cost estimations, since it was assumed that a generator is standard to already be on-site for any hi-tech manufacturing plant in South Africa. Additional cost information regarding utilities, labour and time parameters are provided in 7.4 Appendix 4 Table 7.4.1. It was assumed for safety reasons that one extra operator needed to be added to SPD default labour setup, to in total 2 operators for every unit operation. Except for unit operations in gas compression and air filtration, where one operator was assigned for those units coming into the seed train and another operator for the main bioreactor. This because these units are scheduled to be performed during the same time and assumed to be located in the same room.

Another estimation made for operating costs, are the facility dependent costs, which were based on capital investment parameters (note not operating parameters). The capital investment parameters include maintenance from equipment specific multipliers which was set to SPD default values (based on equipment purchase cost), as well as depreciation and miscellaneous costs. The miscellaneous costs were set to 1% of direct fixed capital (DFC) for insurances, and 2% respective 5% of DFC for local taxes respectively factory expense. It should be noted that the operating cost category waste disposal, was not considered in this project and was set to zero.

The exchange rates used to obtain values in American dollars for SuperPro Designer cost input, are provided in 7.4 Appendix 4 Table 7.4.2. In the case of raw materials, exchange rates from euros were used for WFI. Conversion from South African rand to American dollars, were made for costs of shipping, electricity, cooled and chilled water as well as labour.

3.3.2 T7 RNAP pricing

Three market prices for T7 RNAP could be found, which are provided in Table 3.3.2. From a global commercial lab supplier, a quote was acquired in August 2022, for T7 RNAP 200U/µl with 25000U. To be able to obtain pricing in American dollars per gram, specific enzyme activity 450 000 U/mg T7 RNAP was used that was found in literature [13], as well as exchange rates from South African rand provided in in 7.4 Appendix 4 Table 7.4.2. The second source presented in Table 3.3.2, is from Public Citizen who reported a total price of the amount T7 RNAP required to produce 8 billion doses of mRNA vaccine, which was converted to $136,312 per gram T7 RNAP [5]. Lastly, an article by Ferreira and Petrides, used the price $300 per ml T7 RNAP stock solution [2]. Ferreira and Petrides reports annual consumption of T7 RNAP in weight and volume of their mRNA vaccine process model, which results in the concentration 1000g/L in the stock solution, leading to a price of $300 per gram T7 RNAP [2]. The concentration used in that article was judged to be unrealistic compared to concentrations reported in lab protocols to maximum 8g/L T7 RNAP [9]. Therefore, the pricing from Ferreira and Petrides was not considered further in this work. The price from Public Citizen was chosen for the base case, and the price from the commercial lab supplier was considered in the sensitivity analysis in section 3.4.

Table 3.3.2 Market prices for T7 RNAP from three different sources.

Source	Price [$/g]
Commercial lab supplier	1,988,455
Public Citizen [5]	136,312
Ferreira and Petrides [2]	300

3.4 Sensitivity analysis

A sensitivity analysis was performed in order to determine the effect of macroscale changes in economic parameters, section 3.4.1, and microscale perspective focusing on process parameter changes, section 3.4.2.

3.4.1 Macroscale: economic parameters

Economic calculations were made in the macroscale sensitivity analysis for profitability indicators: gross margin, return on investment (ROI), payback time, net present value (NPV), and internal rate of return (IRR).

3.4.1.1 Profitability analysis

The calculations were based on cash flow analysis data from SPD over 25 years (the project´s lifetime) extracting following: distribution of direct fixed capital, sales revenue, operating cost and depreciation. The timeline was adjusted to 0-24 years, where year 3 marks the start of operation since construction period and start-up time occurs years 0-2, see detailed time and other cost parameters in 7.4 Appendix 4 Table 7.4.1.

Gross profit was calculated by subtracting the cost of sales (operating costs in this case) from sales revenue for each year [47]. Gross profit subtracted by depreciation results in taxable income, and net profit refers to the income after taxes been deducted (tax rate provided in 7.4 Appendix 4 Table 7.4.1) [47]. Net cash flow (NCF) was calculated by deducting direct fixed capital from net profit, which was used to obtain cumulative NCF [47]. Cumulative NCF illustrates when the total of cash flows in the project breaks from negative value to positive [48]. Lastly, discounted NCF was calculated by dividing net cash flow by cost of capital (details are explained with NPV in section 3.4.1.2) [47].

3.4.1.2 Profitability indicators

The gross margin reflects the proportion of sales revenue that results in gross profit, and was calculated based on gross profit and sales revenue from year 3 (in line with SPD calculations) [47]. The ROI measures the net profit (from year 3) as a percentage of total investment (including start-up cost and working capital) [47]. The payback time is the period required to recover investment cost with net cash inflows [47]. It was identified where cumulative NCF reaches start-up cost, starting from operation time (excluding construction period and start-up time), see more details in 4.4.4 Limitations of SuperPro Designer for economic assessment. The NPV measures the present value of all expected NCF for the project, by the sum of discounted NCF, described by equation (4). In equation (4) the project´s lifetime, T, was 24 (since it starts on year 0) and the cost of capital, k, was 7%.

$$NPV = \sum_{t=0}^{T} \frac{NCF_t}{(1+k)^t} \quad (4)$$

An internal rate of return (IRR) was calculated and represent the cost of capital at which the NPV is equal to zero [48].

3.4.1.3 Changed economic parameters

The above profitability indicators were calculated for 20% variations in direct fixed capital, operating cost, and sales revenue. In addition, sales revenue was specifically changed to the price of T7 RNAP from commercial lab supplier due to its large deviation from base case (1359% higher sales revenue than base case). No economic calculations were made for this specific case, instead it was modelled into SPD and economic evaluation reports were extracted from the simulation.

3.4.2 Microscale: process parameters

A microscale sensitivity analysis was done focusing on process parameters to investigate how sensitive the model is to changes in upstream and downstream process related to biomass yield and T7 RNAP yield respectively. The base case was based on yields obtained from Zawadzki *et al* (see Table 3.2.2). The microscale sensitivity analysis aimed to investigate the effect on annual throughput, cost and profitability if other references for yields were used. The microscale sensitivity analysis was performed by changing parameters in the model in SPD. Regarding changes in T7 RNAP yield, different mass coefficients were applied in the homogenization, based on calculations presented in 7.2 Appendix 2 Table 7.2.1, Table 7.2.3, Table 7.2.4. Economic evaluation reports were extracted from SPD simulation. A detailed protocol of what was changed from the base case model, is provided in 7.5 Appendix 5.

4 Results & Discussion

4.1 Process results

The resulting process model can be viewed in Figure 5.

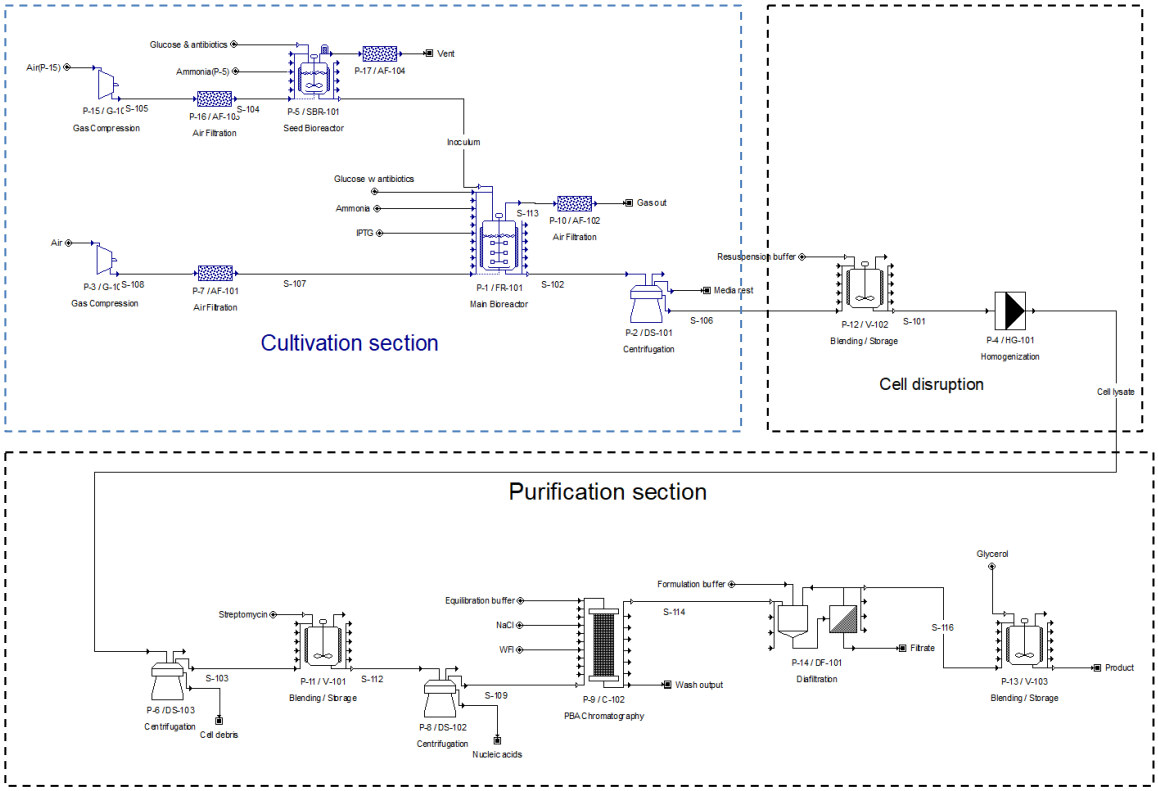

Figure 5 Figure from model file of proposed T7 RNAP process in SuperPro Designer. The blue section of the figure represents the cultivation and upstream process. The black boxes represent the downstream process which includes cell disruption and purification section (which in the figure also include formulation).

The process based on the model was able to obtain 930mg purified T7 RNAP per batch, and each batch took 65 hours and 41 minutes. In order to achieve 38.3g of T7 RNAP as annual throughput (due to software precision limitations 38.3g was achieved instead of the 38.1g that was calculated in 3.2.3), the simulation required 41 batches and an annual operating time of 864 hours and 8 minutes. A full year production is considered to have approximately 8000 operating hours, which indicates this model uses 11% of operating time capacity for the production site [32], [49]. This opens up for several beneficial opportunities, such as producing more T7 RNAP for potential export or using the process equipment to produce other enzymes. It can be of special interest to investigate whether other enzymes required for the mRNA vaccine process (specified in section 2.1) can be produced in the same facility and with same equipment as modelled for T7 RNAP. This would enable larger parts of the mRNA vaccine value chain to be independent in South Africa. It could also be of economic interest to investigate if T7 RNAP production could be located at same facility as mRNA vaccine production. The size of the bioreactors of this model, 15L and 2L, indicates that a relatively small space is required for T7 RNAP production.

Another result from the simulation is the purification yield which represents how well the purification section of the process can recover T7 RNAP. The purification yield was calculated by dividing the amount of T7 RNAP in the product stream by the amount of T7 RNAP in the

stream after the homogenization unit (stream location can be seen in Figure 5). The resulting purification yield for the model was 78%, indicating that 22% of T7 RNAP was lost, which is considered reasonable compared to literature for commercial-scale manufacturing of biopharmaceuticals [50].

4.2 Economic analysis

The cost results from an economic evaluation report extracted from the SPD simulation of the base case, are provided in Table 4.2.1. The capital investment obtained for the base case scenario was $12,786,000, which is less than half of other techno economic analyses of enzyme manufacturing previously conducted [32], [40]. However, the scale of production in referred literature was larger and used 300,000L respective 100,000L bioreactors, compared to this model´s 15L bioreactor, which can indicate a lower equipment cost for this model compared to literature [32], [40]. Operating costs for the T7 RNAP process, $2,399,000, were also lower compared to literature [32], [40]. The cost composition of annual operating costs can be viewed in Figure 6. As Figure 6 presents, facility dependent costs accounted for approximately 95% of the total annual operating costs. Compared to other processes in literature which operates full year, T7 RNAP process operates 11% of the time capacity which is approximately 1.5 months. It can therefore be considered that T7 RNAP process uses less raw materials, utilities, labour and quality work than a process that operates full year. However, annual facility costs such as maintenance, depreciation of equipment and miscellaneous costs e.g. insurances, are likely to be the same for a full year operation and for a process that operates 1.5 months of a year. Detailed costing and usage of raw materials are provided in 7.6 Appendix 6, Table 7.6.1.

The unit production cost for the base case was approximately $62.7 million per kg T7 RNAP, which is considerably lower than market price for T7 RNAP of $136.3 million- or $2 billion per kg T7 RNAP (from Table 3.3.2).

Table 4.2.1 Costs for base case T7 RNAP process.

Total Capital Investment	12,786,000	$
Operating Cost	2,399,000	$/yr
Revenues	5,217,000	$/yr
Net Unit Production Cost	62,689,593.41	$/kg T7 RNAP
Unit Production Revenue	136,312,000.00	$/kg T7 RNAP

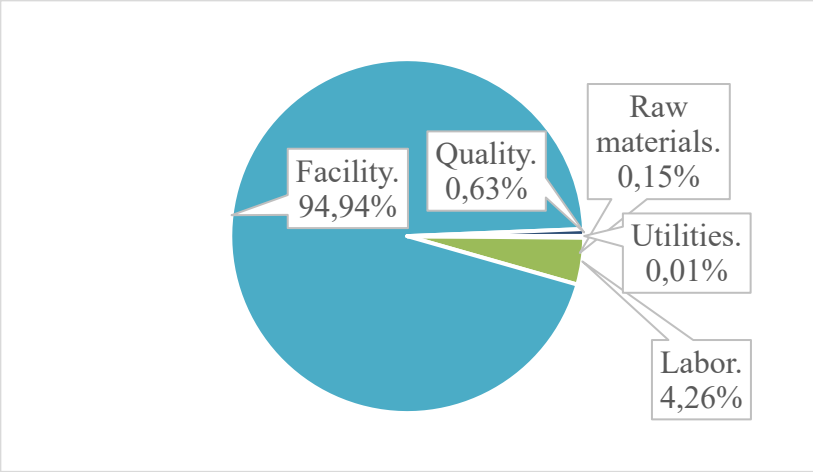

Figure 6 Annual operating costs distribution for base case T7 RNAP process.

Table 4.2.2 shows the profitability indicators of the T7 RNAP process. The gross margin illustrates that the revenues were 54% higher than the operating costs. The ROI was 25.51%, indicating there would be a return on investment already from year 3. With 7% interest (cost of capital) the net present value (NPV) reached $19,250,000. It would require a rate of 21.33% to make the NPV reach zero, (i.e. IRR), which is the highest rate at which the project can break even [48]. As general decision rules a project is considered profitable if the NPV is positive, and the IRR is greater than the entity´s cost of capital [47]. More specifically, in South Africa the average IRR for equities are 15-20.5% and 9-17% for property, which implies this project´s IRR of 21.33% could be a profitable investment [51]. The economic analysis concludes, from all the mentioned profitability indicators, the T7 RNAP process based on this model can be considered profitable.

Table 4.2.2 Profitability indicators of base case T7 RNAP process.

Gross Margin	54.01	%
Return On Investment	25.51	%
Payback Time	3.92	years
IRR (After Taxes)	21.33	%
NPV (at 7.0% Interest)	19,250,000	$

4.3 Sensitivity analysis results

A sensitivity analysis was performed to determine the effect on profitability of macroscale changes in economic parameters, results in section 4.3.1, and microscale perspective focusing on process parameter changes, results in section 4.3.2.

4.3.1 Macroscale: economic parameters changed

Results from the macroscale sensitivity analysis are provided in Table 4.3.1. The analysis conclude that the lowest profitability of the model would be obtained by decrease in revenue, hence the model´s profitability is more sensitive to changes in revenues than direct fixed capital or operating costs. Although, a 20% decrease in direct fixed capital resulted in similar profitability considering IRR, ROI and payback time. To be noted, payback time reported in Table 4.3.1 is not discounted, it was identified where cumulative NCF reaches start-up cost,

starting from operation time, as described in section 3.4.1.2. Considering net present value (NPV), changes in revenue had most impact and second largest impact was caused by operating costs. This is also illustrated in Figure 7, where discounted cash flow is presented, since NPV is the sum of discounted cash flow.

Table 4.3.1 Results of sensitivity analysis with ±20% changes in direct fixed capital (DFC), annual operating cost (OC), and revenue based on the base case

	Base case	**DFC +20%**	**DFC -20%**	**OC +20%**	**OC -20%**	**Revenue +20%**	**Revenue -20%**
NPV (7%) [thousand$]	19254	17014	21493	15777	22730	26814	11693
IRR	21%	18%	26%	19%	23%	26%	16%
ROI	26%	21%	32%	23%	28%	32%	19%
Gross Margin	54%	54%	54%	45%	63%	62%	43%
Payback time [years]	3.92	4.70	3.14	4.41	3.53	3.16	5.16

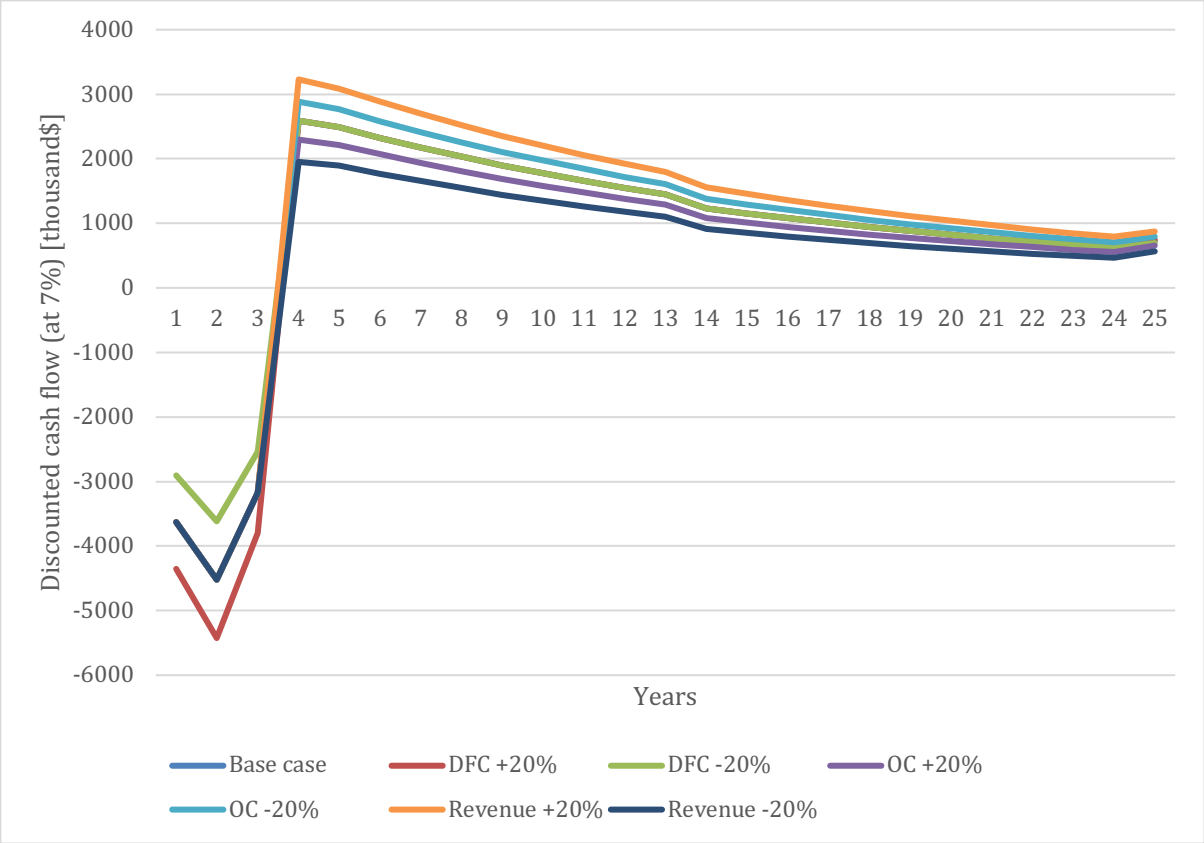

Figure 7 Discounted cash flow (capital of cost 7%) for base case, as well as ±20% change in Direct Fixed Capital (DFC), Operating Costs (OC) and Revenue. Below zero discounted cash flow, base case line is covered by the dark blue line representing revenue -20%. Above zero discounted cash flow, base case line is covered by the green line, DFC -20%.

A specific revenue case based on pricing from a commercial lab supplier ($1,988,455/g T7 RNAP, see Table 3.3.2) was also analysed to determine the effect of choice of T7 RNAP pricing source. This pricing implies a revenue increase of 1359% compared to base case. The NPV was $532 874 000, IRR 148%, ROI 441%, gross margin 97% and payback time 0.23 years. The profitability indicators imply extremely high profitability for this specific T7 RNAP price from a commercial lab supplier.

It was also investigated at what T7 RNAP price the NPV for the suggested T7 RNAP process would reach zero and thereby indicate the process to be non-profitable. This was done to simulate a market price drop of T7 RNAP, in order to identify the T7 RNAP price when it would be more affordable to purchase T7 RNAP externally than to produce with the suggested T7 RNAP process in South Africa. Figure 8, shows that NPV equals zero when the price is $66,849/g T7 RNAP. To be noted, the unit operating cost was $62,690/g T7 RNAP and resulted in a negative NPV. Overall, manufacturing of T7 RNAP in South Africa with the suggested process is more affordable than purchasing externally when the market price is higher than $66,849/g T7 RNAP.

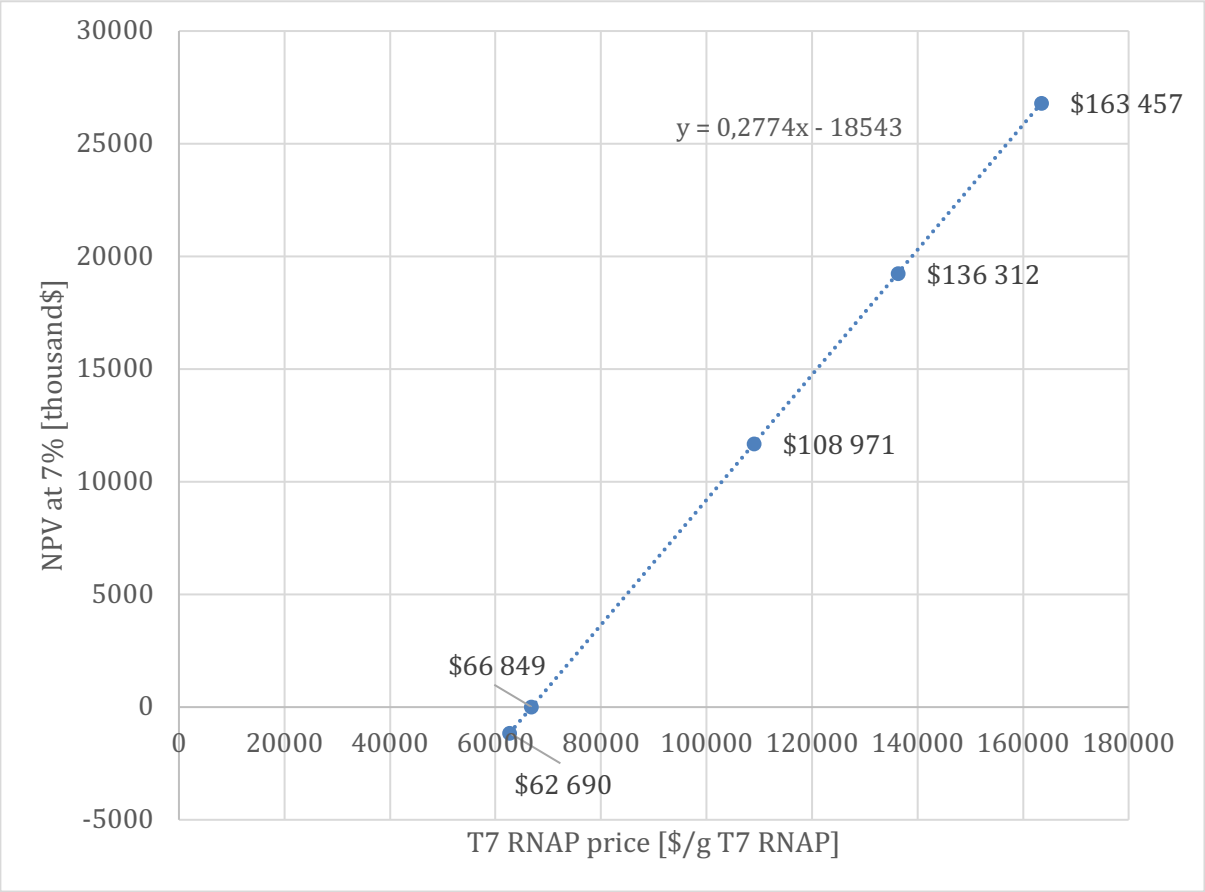

Figure 8 Changes in T7 RNAP price to identify at what price NPV equals zero. Data labels present the T7 RNAP price. NPV for base case (data in Table 4.2.2) and revenue changes ±20% (data in Table 4.3.1) was plotted. NPV for unit operating cost was calculated according to section 3.4.1 (cost in Table 4.2.1). The T7RNAP price when NPV equals zero was obtained from trendline equation.

4.3.2 Microscale: process parameters changed

The microscale sensitivity analysis was performed by adjusting biomass yield (upstream) and T7 RNAP yield (downstream). Section 7.7 Appendix 7 Table 7.7.1 provide detailed parameter changes and results in its entirety of the microscale sensitivity analysis. A summary of the changes for each scenario are provided in Table 4.3.2.

Table 4.3.2 Summary of changes to base case for microscale sensitivity analysis.

Scenario	**Change**	**Reference for change**
A	Downstream: 73% lower T7 RNAP yield	Milligan *et al*, Table 7.2.4
B	Downstream: 14% higher T7 RNAP yield	Composition based, Table 7.2.1
C	Downstream: 33% higher T7 RNAP yield	Davanloo *et al*, Table 7.2.3
D	Upstream only seed bioreactor: 25% higher biomass yield	Davanloo *et al*, Table 3.2.2
E	Upstream both bioreactors: 25% higher biomass yield	Davanloo *et al*, Table 3.2.2
F	Combination Up- & Downstream	Davanloo *et al*, Table 3.2.2 & Table 7.2.3
G	Combination Up- & Downstream	Milligan *et al*, Table 3.2.2 & Table 7.2.4

The NPV from the different scenarios are displayed in Figure 9. Negative NPV, which implies non-profitable project, are obtained by scenario A and G which both has T7 RNAP yield from Milligan *et al*. Milligan *et al* reports a 73% lower T7 RNAP yield, 0.13 mass coefficient for T7 RNAP, compared to the base case where mass coefficient for T7 RNAP was 0.49 (see 7.7 Appendix 7). It should be noted that Milligan *et al* reported the T7 RNAP yield as "at least 30 mg of purified enzyme/liter of cell culture", which indicates that the yield used for the sensitivity analysis could be unnecessarily low as well as the units were presented less reliably than the unit expressed per gram *E.coli*. Milligan *et al* refers to Davanloo *et al* for biomass yield, which was used to convert the yield into desired unit (in 7.2 Appendix 2), even though different *E.coli* strains were reported (see Table 3.2.2). For these reasons, Milligan *et al* can be judged as a less relevant source and scenario A and G could be judged as less likely scenarios to occur.

The sensitivity of T7 RNAP yield can be seen as the gradually increasing NPV with increasing yield (scenario A-C), in Figure 9. Scenario B has 14% higher T7 RNAP yield than base case, while scenario C has 33% higher T7 RNAP yield than base case. The NPV also increased with scenario E which had a 25% increase in biomass yield compared to base case. Hence, both downstream and upstream parameters affect the NPV. The highest NPV is obtained by scenario F which represent the effect if Davanloo *et al* was chosen as a reference for both biomass yield and T7 RNAP yield.

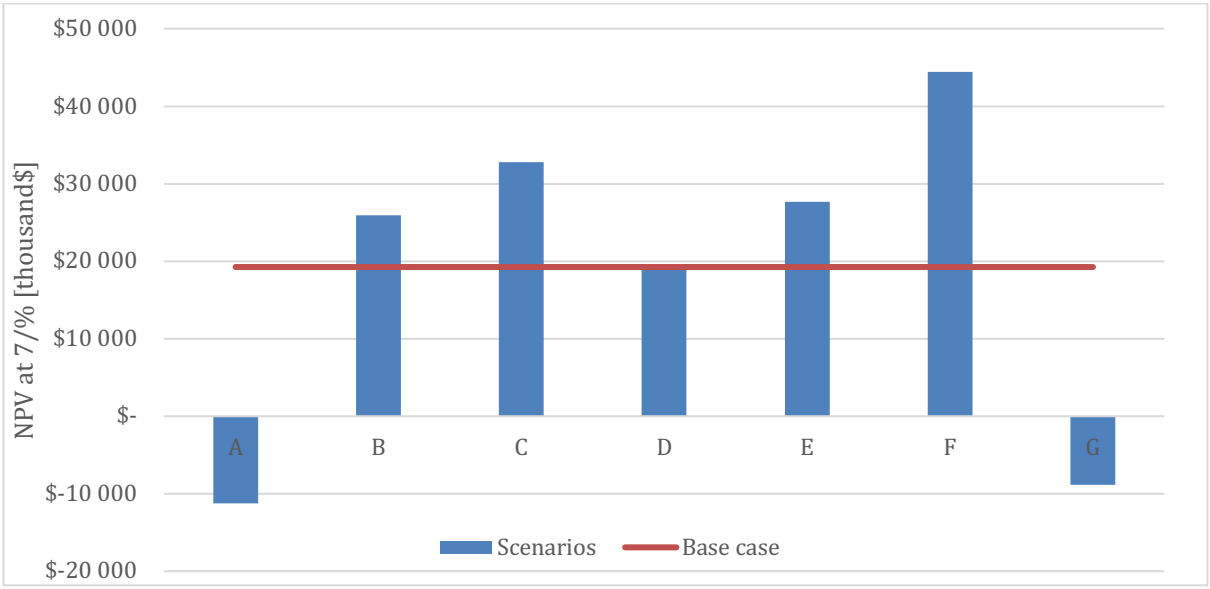

Figure 9 NPV of scenarios A-G, the scenarios are described in Table 4.3.2. The NPV of the base case $19 250 000 is displayed as a red line.

Same trend of profitable and unprofitable scenarios can be seen in IRR and cost reduction, in Figure 10. Cost reduction represent the percentage of how much the scenario´s net unit production cost of T7 RNAP decreased compared to base case. The negative cost reduction for scenario A and G in Figure 10, thereby implies a cost increase. Since the NPV is negative for scenario A and G (as seen in Figure 9), an IRR is not applicable. The highest IRR and cost reduction is obtained by scenario F.

The T7 RNAP yield changes appear to not be linearly connected to the cost reduction. As can be seen in Figure 10, a smaller change in T7 RNAP yield (14%) such as for scenario B corresponds to approximately the same cost reduction (15%). Although larger changes in T7 RNAP yield does not seem to correspond to its cost reduction (A: -73% T7 RNAP yield & -312% cost reduction; B: 33% T7 RNAP yield & 27% cost reduction). The biomass yield change of 25% in scenario E, resulted in a 18% cost reduction. This could indicate that the model is more sensitive to changes in T7 RNAP yield than biomass yield. However, such conclusion should be considered with caution, since only one change in biomass yield was used in the sensitivity analysis.

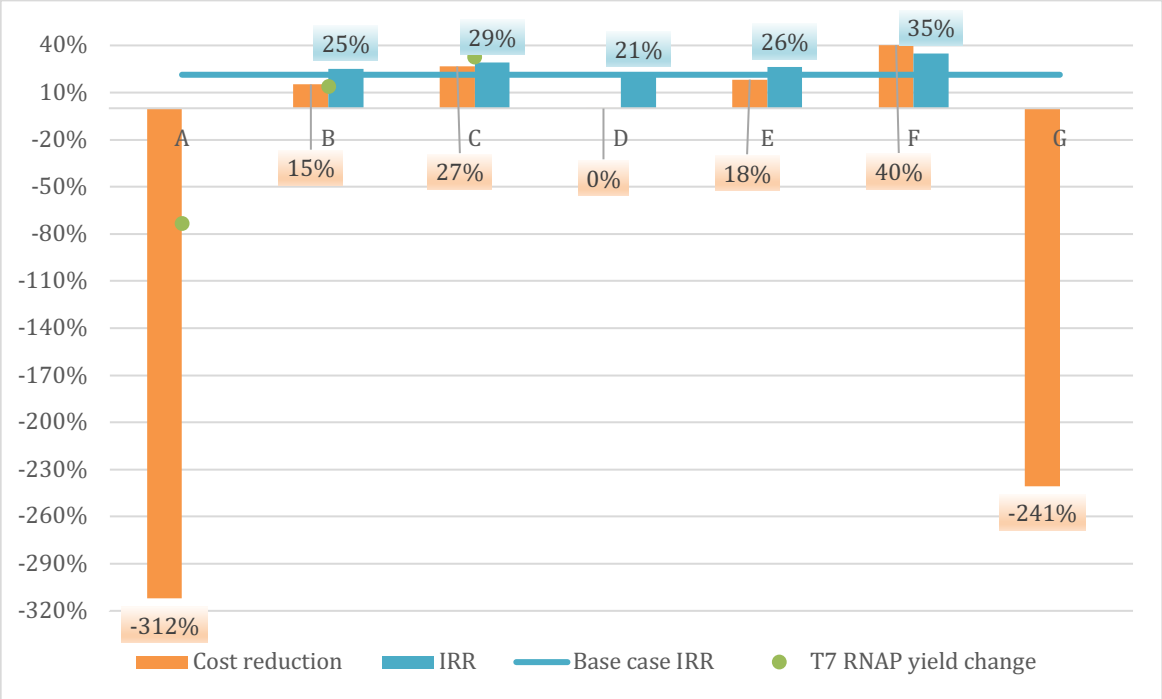

Figure 10 Cost reduction and IRR are displayed for scenarios A-G, the scenarios are explained in Table 4.3.2. The IRR for base case, 21.33%, is presented with a turquoise line. The green dots represent the change of T7 RNAP yield compared to base case.

Furthermore, the different biomass yield used in the microscale sensitivity analysis was reported by Davanloo *et al*. A reliable source for standard biomass yield at industrial scale has been hard to find. Table 4.3.3 presents biomass yields found in literature search. It was of interest to see if there was an increase in biomass yield with more recent published articles, which was disproved by Rosano *et al* and Iram *et al* who reported same or lower biomass yield than used in the model. The biomass yield reported in Horn *et al*, is considered an outlier and could be questioned how such high yield can be obtained, even though the process is fed batch. To be noted though, other technoeconomic analysis have used the biomass yield from Horn *et al* to model an industrial scale production [32]. However, the large variety on biomass yield in Table 4.3.3 indicates more data and research are needed.

Table 4.3.3 Literature research results of biomass yield.

Source	**Wet biomass yield [g *E.coli* /L culture]**	**Dry biomass yield* [g dry *E.coli*/L culture]**	**Growth media details**
Davanloo *et al* (1984) [8]	10	3.0	M9 TB
Milligan *et al* (1989) [10]	10**	3.0	M9 TB**
Zawadzki *et al* (1991) [12]	8	2.4	M9 TB
Horn *et al* (1996) [52]	-	80-120	Fed batch
Marisch *et al* (2013) [53]	-	17.4	High glucose concentration: 40g/L
Rosano *et al* (2014) [54]	-	3	LB
Iram *et al* (2021) [55]	3.5	1.05	LB
Internal experience reported from laboratory at Stellenbosch University (2022) [56]	17	5.1	TB, 0.1mM IPTG

* When wet biomass yield has been reported it has been converted to dry biomass yield by multiplying with 0.3 (since 70% of *E.coli* is composed of water according to Table 3.2.1).
**Refers to Davanloo *et al.*

Additional results of the microscale sensitivity analysis are shown in Figure 11, where scenario F is the scenario were most T7 RNAP was produced. In the three Figure 9Figure 11, it is illustrated that scenario D does not differ much from base case, which could be explained by the main bioreactor still controlled the biomass yield output to the rest of the process.

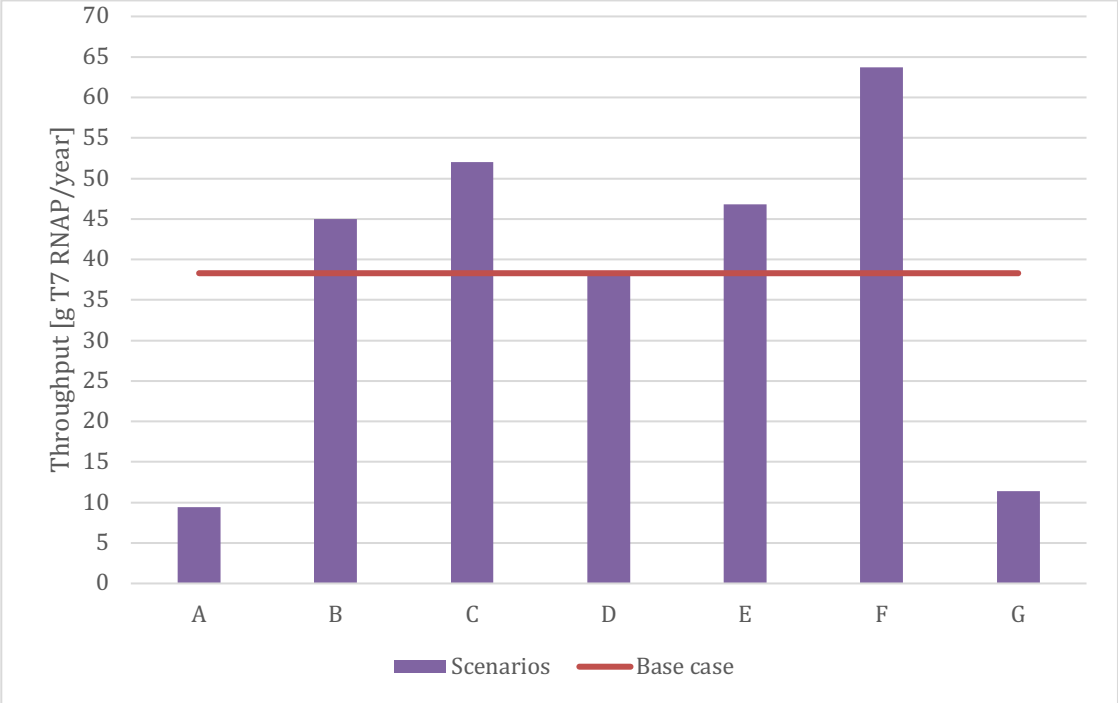

Figure 11 Annual throughput of T7 RNAP possible with different sensitivity scenarios A-G, the scenarios are explained in Table 4.3.2.

To summarize the results of the microscale sensitivity analysis, the model is sensitive to both biomass yield changes and T7 RNAP yield. The largest impact on profitability is an increase of both biomass yield and T7 RNAP yield.

4.4 Result validity

Some uncertainties of the model are emphasized in this section to give transparency and to evaluate the validity of the results.

4.4.1 Scale and yields

Firstly, the model in this project has been based on lab protocols since there have been no publicly available data on industrial scale. Adjustments have been made such as recalculating column size instead of scaling up, since it is well known that in lab environments it is more common to use the equipment size available instead of what is required for the process. Still, this model can differ compared to industrial production in practice.

Especially, the T7 RNAP yield and biomass yield used for the model that are based on lab scale. The process is mainly based on a lab protocol from Rues *et al* (2016) which was considered to provide the most clear and relevant production steps for a modern production, while the yields were obtained by Zawadzki *et al* from 1991. The two lab protocols differ in their T7 RNAP preparation. As mentioned in section 3.2.2.1, Zawadzki *et al* reports another type of cell disruption method than Rues *et al,* and it can thereby be questioned if the data from Zawadzki *et al* should have been used in the model. Although, due to lack of published data on

T7 RNAP yield, and that another cell disruption method was used in the model to adjust for industrial scale, the yields from Zawadzki *et al* can be judged as sufficient. In addition, the same strains and plasmids were used by Rues *et al* and Zawadzki *et al*, which was considered an important factor and strengthens its compatibility. Other sources than Zawadzki *et al* reporting T7 RNAP yield were considered in the sensitivity analysis. The T7 RNAP yield selected for the base case can be considered as a conservative choice, since Zawadzki *et al* had the second lowest T7 RNAP yield reported after Milligan *et al*, out of the four options presented in 7.2 Appendix 2. However, to gain more accurate and modern yields, further research needs to be performed. Since the yield data in the model were from 1991, it could be argued that higher T7 RNAP yields and biomass yields are expected in a modern industrial scale production.

Due to higher T7 RNAP yield could be expected than reported from the sources, the purification yield 77% was accepted for the model calculations in 7.2 Appendix 2, even though a 78% purification yield was obtained once the values were inserted to the model. This difference of purification yield indicates that approximately 2% higher amount of T7 RNAP was modelled for the base case than what was reported in Zawadzki *et al*.

4.4.2 Annual throughput

Estimations made for future demand of T7 RNAP to calculate the annual throughput is another element of uncertainty, which is described in section 3.2.3. The annual throughput mainly affects the result of annual operating time, which is one of the main interesting results due to the opportunities the few operating hours lead to. Firstly, the estimations were based on solely mRNA vaccine demand of T7 RNAP, even though T7 RNAP can be used for other applications as well, as stated in section 1.1. Therefore, the demand for South African T7 RNAP could be higher than the estimated 38g. Secondly, the demand could also be higher if also vaccines for Sub-Saharan Africa were considered.

On the contrary, less T7 RNAP demand could be possible since the estimation is based on the required amount of T7 RNAP for Moderna´s mRNA COVID vaccine. Pfizer´s mRNA vaccine for COVID required 70% less T7 RNAP amount than Moderna, which is described in section 2.1. However, Afrigen in Cape Town, which is part of the mRNA vaccine technology transfer hub funded by WHO, uses the sequence of Moderna´s mRNA COVID vaccine [57]. Therefore, Moderna´s required amount for T7 RNAP was the most interesting for the estimation. Although, it was assumed that the same amount of T7 RNAP would be required for two other mRNA vaccines covering other diseases than COVID, such as Zika and influenza. Furthermore, it could be discussed if the South African vaccination rate for COVID could be transferred to three different vaccine doses taken annually per South African as the estimation is based on. The vaccination rate could be less which would lead to less annual T7 RNAP demand than 38g.

However, the arguments for lower annual throughput could weigh out the arguments for a higher amount than 38g of T7 RNAP. It should be noted that to establish the mRNA vaccine technology as Afrigen does, less T7 RNAP would be required than to support the entire South African mRNA vaccine manufacturing demand which this project aims to [4]. If smaller annual throughput is desired, the equipment size of the model can still be relevant, although the annual operating time would be less and can be calculated based on the batch size and batch time provided in section 4.1.

4.4.3 Cost estimations

The economic results such as the costs and profitability of the suggested T7 RNAP process, is affected by the cost estimations made. There are several cost estimations that could be higher cost than used. First and foremost, the shipping cost based on an DHL tariff guide for export from South Africa, could be higher since importing to South Africa is generally known to be more expensive than exporting. Although, that difference could have been covered by the added VAT and customs fees. Moreover, the raw material price could be higher since pharma grade could not be ensured for all raw materials from the sources. Streptomycin sulphate pricing was obtained by Sigma and was explicitly not intended for pharmaceutical production, therefore higher price could be expected. Nevertheless, Sigma is generally known to provide material for lab scale. As seen in appendix 6, streptomycin sulphate is responsible for 47% of the raw materials cost, which could indicate the streptomycin sulphate price was obtained from an unreliable source for cost estimations on industrial scale. Overall, the raw material prices are responsible for 0.15% of the annual operating cost (see Figure 6), and thereby the obtained price data for raw materials can be judged as sufficient for this project.

The electricity cost, in the category utilities, should be higher than used in the model. The electricity cost was based on an energy charged per kWh and a service fee charged per day, as can be seen in 7.4 Appendix 4 Table 7.4.1. The latter was converted to being charged per kWh as well for modelling purposes. The electricity cost was calculated based on data during model development and concluded the price $2.13/kWh. Although, when the base case was finalized, the results would lead to a price for electricity of $3.75/kWh. In practise the electricity usage could also be expected to be higher but less glycol usage. This is because glycol was used as cooling agent for centrifuges, high-pressure homogenization and diafiltration, while equipment in industrial scale is expected to have a pre-cooling function which is assumed to use electricity, as mentioned in section 3.2.4. It could also be argued that higher electrical usage could be expected from a cold room which is expected to be at the facility. Although the cold room cost could be considered included in the electrical facility cost which is part of the direct fixed capital, see 7.4 Appendix 4 Table 7.4.3. However, the potential changes mentioned for electrical cost are considered to not affect the economic results significantly since the utilities costs are responsible for 0.01% of the total operating costs.

4.4.4 Limitations of SuperPro Designer for economic assessment

The limitations of SPD have also affected the validity of the economic assessment. One limitation of SPD identified when viewing a cash flow report extracted from SPD, is that the sales revenue has the same value for every operating year. Hence, it does not take into future value calculation based on interest rate. Another limitation identified regarding the sales revenue, is that the revenue shown in table 4.2.1, is 0.1% less than what is accurate. The actual revenue should be $5,221,000 when the pricing from T7 RNAP is converted to sales revenue with annual throughput.

Further on in the cash flow report, the years presented in the profitability analysis table was 1 to 25, instead of starting with year 0 (0-24), which is required to achieve accurate calculations for NPV. However, the year values (1-25) presented in the profitability analysis table are solely a confusion for the SPD user, since SPD reports an accurate NPV based on year 0-24. Although the NPV and IRR are imprecise since the start-up cost has not been considered in the net cash flow, which is required in the formula (see equation (4) in section 3.4.1.2). Nonetheless, when controlling the calculations for payback time it was noted that the start-up cost is included in

the cumulative net cash flow (not presented in the cash flow report from SPD), which indicates that payback time reported is precise and trustworthy.

4.5 Production in South Africa

Despite the uncertainties discussed in section 4.4, the T7 RNAP process could be considered profitable, as described in section 0. In more detail, the suggested process can produce T7 RNAP for a production cost of approximately $63 million per kg, while it is bought from external suppliers for approximately $136 million or $2 billion (per kg T7 RNAP), as presented in section 3.3.2. The enormous difference between production cost and external selling price should indicate large savings for South African mRNA vaccine manufacturers if they would produce T7 RNAP themselves. It can thereby be questioned why there is no current T7 RNAP manufacturing in South Africa.

One reason could be that South Africa lacks stakeholders that are willing to or have the capacity to fund the initial capital investment, of $12,786,000 for the suggested T7 RNAP process. It could be related to the risks involved to start-up a GMP manufacturing facility in South Africa. One such risk could be slow regulatory approval which can be expected due to the reported backlog in medicines registration at South African Health Products Regulatory Authority (SAHPRA) [58]. Another potential risk could be related to shipment and long waiting time for material and equipment required to build the facility and process. On the contrary, the waiting time could also be applied to receive raw materials for the mRNA vaccine manufacturing causing delays in the production. Hence, to optimize the mRNA vaccine production it is beneficial to produce T7 RNAP locally.

Moreover, the labour in South Africa can be considered more affordable than for instance in Europe, which contributes to lower construction and production cost. However, to construct and run a GMP manufacturing plant specific skilled expertise is required, which there can be a shortage of in South Africa. Power outages and thereby interruption in power supply to the process could be considered another disadvantage for South African production, even though generators and batch process (like this project modelled) can partly solve that problem.

It should be emphasized though, that one main reason to why there is no current T7 RNAP manufacturing in South Africa could be that the mRNA vaccine technology is relatively new, as mentioned in section 1.1. The demand of T7 RNAP increases at the moment with the development of mRNA vaccine production in South Africa.

5 Conclusion

The results indicated that South African T7 RNA polymerase production is profitable and feasible. The hypothesis proved to be correct, with approximately 50% lower unit production cost for South African production of T7 RNAP than purchasing it externally for the base case.

South African annual demand for T7 RNAP to mRNA vaccine production is fulfilled by operating approximately 1.5months a year with the suggested 15L main bioreactor used in this model. Thereby, it is recommended to further investigate the possibilities to manufacture other required enzymes for mRNA vaccine production to enable an independent value chain for South Africa.

The economic assessment is most sensitive to changes in revenue, indicating much higher profitability with increased T7 RNAP price. The model proved to be sensitive also to changes in process parameters of both biomass yield and T7 RNAP yield.

6 References

[1] S. S. Rosa, D. M. F. Prazeres, A. M. Azevedo, and M. P. C. Marques, "mRNA vaccines manufacturing: Challenges and bottlenecks," *Vaccine*, vol. 39, no. 16, pp. 2190–2200, Apr. 2021, doi: 10.1016/j.vaccine.2021.03.038.

[2] R. Ferreira and D. Petrides, *Messenger RNA (mRNA) Vaccine Large Scale Manufacturing – Process Modeling and Techno-Economic Assessment (TEA) using SuperPro Designer.* 2021. doi: 10.13140/RG.2.2.34118.80966.

[3] "What is Africa's vaccine production capacity?," *WHO | Regional Office for Africa*. https://www.afro.who.int/news/what-africas-vaccine-production-capacity (accessed Aug. 09, 2022).

[4] "The mRNA vaccine technology transfer hub." https://www.who.int/initiatives/the-mrna-vaccine-technology-transfer-hub (accessed Aug. 09, 2022).

[5] Public Citizen, "How to Make Enough Vaccine for the World in One Year." https://www.citizen.org/article/how-to-make-enough-vaccine-for-the-world-in-one-year/ (accessed Aug. 09, 2022).

[6] X. Liang, C. Li, W. Wang, and Q. Li, "Integrating T7 RNA Polymerase and Its Cognate Transcriptional Units for a Host-Independent and Stable Expression System in Single Plasmid," *ACS Synth. Biol.*, vol. 7, no. 5, pp. 1424–1435, May 2018, doi: 10.1021/acssynbio.8b00055.

[7] R. Sousa, "T7 RNA Polymerase," in *Encyclopedia of Biological Chemistry*, W. J. Lennarz and M. D. Lane, Eds. New York: Elsevier, 2004, pp. 147–151. doi: 10.1016/B0-12-443710-9/00240-4.

[8] P. Davanloo, A. H. Rosenberg, J. J. Dunn, and F. W. Studier, "Cloning and expression of the gene for bacteriophage T7 RNA polymerase," *Proc. Natl. Acad. Sci. U. S. A.*, vol. 81, no. 7, pp. 2035–2039, Apr. 1984, doi: 10.1073/pnas.81.7.2035.

[9] R.-B. Rues, E. Henrich, C. Boland, M. Caffrey, and F. Bernhard, "Cell-Free Production of Membrane Proteins in Escherichia coli Lysates for Functional and Structural Studies," in *Heterologous Expression of Membrane Proteins: Methods and Protocols*, I. Mus-Veteau, Ed. New York, NY: Springer, 2016, pp. 1–21. doi: 10.1007/978-1-4939-3637-3_1.

[10] J. F. Milligan and O. C. Uhlenbeck, "Synthesis of small RNAs using T7 RNA polymerase," in *Methods in Enzymology*, vol. 180, Academic Press, 1989, pp. 51–62. doi: 10.1016/0076-6879(89)80091-6.

[11] D. Schwarz *et al.*, "Preparative scale expression of membrane proteins in Escherichia coli-based continuous exchange cell-free systems," *Nat. Protoc.*, vol. 2, no. 11, Art. no. 11, Nov. 2007, doi: 10.1038/nprot.2007.426.

[12] V. Zawadzki and H. J. Gross, "Rapid and simple purification of T7 RNA polymerase," *Nucleic Acids Res.*, vol. 19, no. 8, p. 1948, Apr. 1991, doi: 10.1093/nar/19.8.1948.

[13] Y. Li, E. Wang, and Y. Wang, "A modified procedure for fast purification of T7 RNA polymerase," *Protein Expr. Purif.*, vol. 16, no. 2, pp. 355–358, Jul. 1999, doi: 10.1006/prep.1999.1083.

[14] E. Henrich, F. Löhr, J. Mezhyrova, A. Laguerre, F. Bernhard, and V. Dötsch, "Chapter Six - Synthetic Biology-Based Solution NMR Studies on Membrane Proteins in Lipid Environments," in *Methods in Enzymology*, vol. 614, A. J. Wand, Ed. Academic Press, 2019, pp. 143–185. doi: 10.1016/bs.mie.2018.08.019.

[15] R. Schnieders *et al.*, "NMR Spectroscopy of Large Functional RNAs: From Sample Preparation to Low-Gamma Detection," *Curr. Protoc. Nucleic Acid Chem.*, vol. 82, no. 1, p. e116, 2020, doi: 10.1002/cpnc.116.

[16] K. Yue, J. Jiang, P. Zhang, and L. Kai, "Functional Analysis of Aquaporin Water Permeability Using an Escherichia coli-Based Cell-Free Protein Synthesis System," *Front. Bioeng. Biotechnol.*, vol. 8, p. 1000, 2020, doi: 10.3389/fbioe.2020.01000.
[17] J. Grodberg and J. J. Dunn, "ompT encodes the Escherichia coli outer membrane protease that cleaves T7 RNA polymerase during purification," *J. Bacteriol.*, vol. 170, no. 3, pp. 1245–1253, Mar. 1988, doi: 10.1128/jb.170.3.1245-1253.1988.
[18] A.-L. Fuchs, A. Neu, and R. Sprangers, "A general method for rapid and cost-efficient large-scale production of 5′ capped RNA," *RNA*, vol. 22, Jul. 2016, doi: 10.1261/rna.056614.116.
[19] C. S. Lee and P. X. Guo, "Tracking and Elimination of an Interfering Polypeptide Coexpressed with the Vaccinia Virus mRNA Capping Enzyme Overproduced in Escherichia coli," *Protein Expr. Purif.*, vol. 4, no. 2, pp. 114–119, Apr. 1993, doi: 10.1006/prep.1993.1017.
[20] J. Whitley *et al.*, "Development of mRNA manufacturing for vaccines and therapeutics: mRNA platform requirements and development of a scalable production process to support early phase clinical trials," *Transl. Res.*, vol. 242, pp. 38–55, Apr. 2022, doi: 10.1016/j.trsl.2021.11.009.
[21] FDA, "CBER assessment of a single booster dose of the Moderna COVID-19 Vaccine (0.25 mL) administered at 5 months." US Food & Drug administration. Accessed: Sep. 14, 2022. [Online]. Available: https://www.fda.gov/media/155548/download
[22] X.-M. Sun *et al.*, "Downregulation of T7 RNA polymerase transcription enhances pET-based recombinant protein production in Escherichia coli BL21 (DE3) by suppressing autolysis," *Biotechnol. Bioeng.*, vol. 118, no. 1, pp. 153–163, 2021, doi: 10.1002/bit.27558.
[23] R. Häuser *et al.*, "Bacteriophage Protein–Protein Interactions," *Adv. Virus Res.*, vol. 83, pp. 219–298, 2012, doi: 10.1016/B978-0-12-394438-2.00006-2.
[24] F. W. Studier and B. A. Moffatt, "Use of bacteriophage T7 RNA polymerase to direct selective high-level expression of cloned genes," *J. Mol. Biol.*, vol. 189, no. 1, pp. 113–130, May 1986, doi: 10.1016/0022-2836(86)90385-2.
[25] C. Szpirer and P. Gabant, "Protein Bioproduction without Antibiotics," *GEN - Genetic Engineering and Biotechnology News*, Oct. 17, 2011. https://www.genengnews.com/magazine/168/protein-bioproduction-without-antibiotics/ (accessed Aug. 31, 2022).
[26] T. Kroemer, "How Does IPTG Induction Work?" Goldbio. Accessed: Aug. 30, 2022. [Online]. Available: https://www.goldbio.com/articles/article/how-does-iptg-induction-work#_Toc56514562
[27] P. M. Doran, *Bioprocess Engineering Principles*. Academic Press, 2012.
[28] S. A. Rouf, P. L. Douglas, M. Moo-Young, and J. M. Scharer, "Computer simulation for large scale bioprocess design," *Biochem. Eng. J.*, vol. 8, no. 3, pp. 229–234, Oct. 2001, doi: 10.1016/S1369-703X(01)00112-7.
[29] P. M. Doran, "Chapter 12 - Homogeneous Reactions," in *Bioprocess Engineering Principles (Second Edition)*, P. M. Doran, Ed. London: Academic Press, 2013, pp. 599–703. doi: 10.1016/B978-0-12-220851-5.00012-5.
[30] R. Ismail, Z. N. Allaudin, and M.-A. M. Lila, "Scaling-up recombinant plasmid DNA for clinical trial: Current concern, solution and status," *Vaccine*, vol. 30, no. 41, pp. 5914–5920, Sep. 2012, doi: 10.1016/j.vaccine.2012.02.061.
[31] C.-J. Huang, H. Lin, and X. Yang, "Industrial production of recombinant therapeutics in Escherichia coli and its recent advancements," *J. Ind. Microbiol. Biotechnol.*, vol. 39, no. 3, pp. 383–399, Mar. 2012, doi: 10.1007/s10295-011-1082-9.
[32] R. da G. Ferreira, A. R. Azzoni, and S. Freitas, "Techno-economic analysis of the industrial production of a low-cost enzyme using E. coli: the case of recombinant β-

glucosidase," *Biotechnol. Biofuels*, vol. 11, no. 1, p. 81, Mar. 2018, doi: 10.1186/s13068-018-1077-0.
[33] D. Herbert and H. L. Kornberg, "Glucose transport as rate-limiting step in the growth of Escherichia coli on glucose.," *Biochem. J.*, vol. 156, no. 2, pp. 477–480, May 1976.
[34] "Agilent Genomics : Tools - Bio Calculators." https://www.agilent.com/store/biocalculators/calcODBacterial.jsp?_requestid=223375 (accessed Oct. 14, 2022).
[35] "ECMDB: ECMDB Statistics." https://ecmdb.ca/e_coli_stats (accessed Sep. 13, 2022).
[36] "Cell_Disruption_by_Homogenization_3006_01_06_2008_US.pdf." Accessed: Oct. 06, 2022. [Online]. Available: http://www.apvhemisan.com/uploads/images/Cell_Disruption_by_Homogenization_3006_01_06_2008_US.pdf
[37] "Cytiva, Sepharose Fast Flow ion exchange resins and prepacked column formats, ION EXCHANGE CHROMATOGRAPHY." Accessed: Sep. 09, 2022. [Online]. Available: https://cdn.cytivalifesciences.com/api/public/content/digi-12944-pdf
[38] S. S. Africa, "60,6 million people in South Africa | Statistics South Africa." https://www.statssa.gov.za/?p=15601 (accessed Oct. 07, 2022).
[39] "South Africa Coronavirus COVID-19 Vaccination Rate - October 2022 Data." https://tradingeconomics.com/south-africa/coronavirus-vaccination-rate (accessed Oct. 07, 2022).
[40] R. Da Gama Ferreira and D. Petrides, "(PDF) Industrial Enzymes Production - Process Modeling and Techno-Economic Assessment (TEA) using SuperPro Designer." https://www.researchgate.net/publication/341102798_Industrial_Enzymes_Production_-_Process_Modeling_and_Techno-Economic_Assessment_TEA_using_SuperPro_Designer (accessed Oct. 17, 2022).
[41] "chemicals, chemicals Suppliers and Manufacturers at Alibaba.com." https://www.alibaba.com/Chemicals_p8?spm=a2700.8293689.allinfo.d8.2ce267afOCJRHo&tracelog=ICBU_PC_HOME_BANNER_LEFT (accessed Oct. 17, 2022).
[42] Seider, Seader, Lewin, and Widagdo, *Product and Process Design Principles*, 3rd ed. John Wiley & Sons, Inc., 2009.
[43] "Inflation, consumer prices (annual %) | Data." https://data.worldbank.org/indicator/FP.CPI.TOTL.ZG?end=2021&start=1960&view=chart (accessed Oct. 11, 2022).
[44] "Streptomycin sulfate salt -." https://www.sigmaaldrich.com/ZA/en/substance/streptomycinsulfatesalt728693810740 (accessed Oct. 11, 2022).
[45] DHL, "DHL Express. Tariff guide 2022." POSTNET Stellenbosch Eikestad store.
[46] "Value-Added Tax | South African Revenue Service," Feb. 04, 2021. https://www.sars.gov.za/types-of-tax/value-added-tax/ (accessed Sep. 19, 2022).
[47] J. Birt, K. Chalmers, S. Maloney, A. Brooks, and J. Oliver, *Accounting: Business Reporting for Decision Making, 6th Edition | Wiley*, 6th ed. Wiley, 2018. Accessed: Nov. 12, 2022. [Online]. Available: https://www.wiley.com/en-us/Accounting%3A+Business+Reporting+for+Decision+Making%2C+6th+Edition-p-9780730362951
[48] R. Turton, R. C. Bailie, W. B. Whiting, and J. A. Shawiqitz, *Analysis, Synthesis, and Design of Chemical Processes, Third Edition [Book]*, 3rd ed. Pearson Education Inc., 2009.
[49] S. Diab, N. Mytis, A. G. Boudouvis, and D. I. Gerogiorgis, "Process modelling, design and technoeconomic Liquid–Liquid Extraction (LLE) optimisation for comparative evaluation of batch vs. continuous pharmaceutical manufacturing of atropine," *Comput. Chem. Eng.*, vol. 124, pp. 28–42, May 2019, doi: 10.1016/j.compchemeng.2018.12.028.

[50] R. A. Rader and E. S. Langer, “Biopharmaceutical Manufacturing: Historical and Future Trends in Titers, Yields, and Efficiency in Commercial-Scale Bioprocessing,” *Bioprocess. J.*, vol. 13, no. 4, pp. 47–54, Winter 2014.
[51] “Net Present Value and Internal Rate of Return,” *Vertical Spaces*, Nov. 15, 2016. https://www.verticalspaces.co.za/news/net-present-value-and-internal-rate-of-return/ (accessed Nov. 14, 2022).
[52] U. Horn *et al.*, “High volumetric yields of functional dimeric miniantibodies in Escherichia coli, using an optimized expression vector and high-cell-density fermentation under non-limited growth conditions,” *Appl. Microbiol. Biotechnol.*, vol. 46, no. 5–6, pp. 524–532, Dec. 1996, doi: 10.1007/s002530050855.
[53] K. Marisch *et al.*, “A Comparative Analysis of Industrial Escherichia coli K–12 and B Strains in High-Glucose Batch Cultivations on Process-, Transcriptome- and Proteome Level,” *PLoS ONE*, vol. 8, no. 8, p. e70516, Aug. 2013, doi: 10.1371/journal.pone.0070516.
[54] G. L. Rosano and E. A. Ceccarelli, “Recombinant protein expression in Escherichia coli: advances and challenges,” *Front. Microbiol.*, vol. 0, 2014, doi: 10.3389/fmicb.2014.00172.
[55] I. Shahzadi *et al.*, “Scale-up fermentation of Escherichia coli for the production of recombinant endoglucanase from Clostridium thermocellum,” *Sci. Rep.*, vol. 11, no. 1, Art. no. 1, Mar. 2021, doi: 10.1038/s41598-021-86000-z.
[56] R. Vermeulen, “Personal Communication,” Aug. 30, 2022.
[57] W. Roelf, “In world first, South Africa’s Afrigen makes mRNA COVID vaccine using Moderna data,” *Reuters*, Feb. 04, 2022. Accessed: Nov. 16, 2022. [Online]. Available: https://www.reuters.com/world/africa/world-first-safricas-afrigen-makes-mrna-covid-vaccine-using-moderna-data-2022-02-03/
[58] A. Keyter, S. Banoo, S. Salek, and S. Walker, “The South African Regulatory System: Past, Present, and Future,” *Front. Pharmacol.*, vol. 9, 2018, Accessed: Nov. 21, 2022. [Online]. Available: https://www.frontiersin.org/articles/10.3389/fphar.2018.01407
[59] V. M. Cardoso *et al.*, “Cost analysis based on bioreactor cultivation conditions: Production of a soluble recombinant protein using Escherichia coli BL21(DE3),” *Biotechnol. Rep.*, vol. 26, p. e00441, Jun. 2020, doi: 10.1016/j.btre.2020.e00441.
[60] N. Herold, “Cost Review of Water For Injection (WFI) Systems | MECO,” *Meco*. https://www.meco.com/cost-review-of-wfi-systems/ (accessed Oct. 11, 2022).
[61] Stellenbosch University, “Design Project, consumable prices (2022).”
[62] Electricity Generation and Distribution Department, “City of Cape Town Link,” *City of Cape Town*. https://www.capetown.gov.za/Work%20and%20business/Commercial-utility-services/Commercial-electricity-services/the-cost-of-electricity#Heading1 (accessed Oct. 11, 2022).
[63] “South Africa Average Monthly Wages in Manufacturing - 2022 Data - 2023 Forecast.” https://tradingeconomics.com/south-africa/wages-in-manufacturing (accessed Oct. 11, 2022).
[64] “South Africa Inflation Rate - September 2022 Data - 1968-2021 Historical.” https://tradingeconomics.com/south-africa/inflation-cpi (accessed Oct. 13, 2022).

7 Appendices

7.1 Appendix 1 Media and main process parameters

Input raw materials for main bioreactor (P-1): was inoculum (0.1L from seed bioreactor P-5), glucose, kanamycin, IPTG, ammonia, air, and water for injection (WFI). Ammonia and air were added in excess, 13% respective 111% above the stochiometric amount for main bioreactor. In the seed bioreactor, ammonia was added 48% in excess while oxygen 148% above the stochiometric amount. Details for other input raw materials are provided in Table 7.7.1.

Table 7.1.1 Media used in the T7 RNAP production. Concentrations were based on Rues et al (dialysis buffer from the reference is here called formulation buffer), except for Kanamycin sulphate which was based on Li et al. Mass composition was calculated.

Component	**Resuspension buffer**		**Equilibration buffer**		**Formulation buffer**		**Others**
	Concentration	Mass composition %	Concentration	Mass composition %	Concentration	Mass composition %	
Tris-HCl	30mM	0.47	30mM	0.47			
EDTA Disodium	10mM	0.33	1mM	0.03	0.5mM	0.02	
Sodium chloride	50mM	0.29	50mM	0.29	10mM	0.06	500mM for chromatograph input stream
Glycerol	5%	5.01	5%	5.00	5%	5.00	
β-mercaptoethanol	10mM	0.08	10mM	0.08			
WFI (Water for Injection)		93.82		94.13		94.74	
Dipotassium phosphate					10mM	0.17	

DTT					1mM	0.02	
IPTG							1mM*
Glucose							Variable**
Kanamycin sulphate							100mg/L***
Streptomycin sulphate in WFI							3% (w/v) ****

*Concentration given with respect to a final concentration of solution in bioreactor, by modelling IPTG as last input of raw materials with 'Pull In' function, 'set by specification' to set final composition for IPTG to 1mM. Input stream concentration of IPTG was 1M.

**Concentration chosen so that the glucose conversion was equal to 95-100%.

***Concentration given with respect to volume of glucose stream.

**** Concentration given with respect to a final concentration of solution in tank, by using the same approach as for IPTG. Input stream concentration of streptomycin sulphate was 30% (w/v).

Table 7.1.2 Main process parameters.

Parameter	Value	Source
Gas compression P-3, P-15		
Process time	0.001h	Defined
Air filtration P-7, P-10, P-16, P-17		
Process time	0.001h	Defined
Seed bioreactor P-5		
Reaction time	10h	Adjusted from [59]
Temperature	37.0°C	[59]
Target concentration of biomass	2.4g/L*	[12]
Bioreactor P-1		
Reaction time	10h	[9], [15]
Temperature	37.0°C	[9]
Target concentration of biomass	2.4g/L*	[12]
Centrifugation P-2		
Sedimentation Efficiency	30%	Defined
Biomass to solids stream	100%	Defined
Solid Concentration in Heavy Stream	120 g/L	Defined
Exit Temperature	4°C	[9]
Centrifugation time	15min	[9]
Homogenization P-4		
Number of Passes	5	[15]
Pressure Drop	15,000 psi	[15]
Homogenization time	360 min	Defined
Cell Disruption	100%	[32]
Temperature	4°C	[15]
Centrifugation P-6		
Sedimentation Efficiency	30%	[32]
Cell Debris Removal	100%	Defined
Solid Concentration in Heavy Stream	200 g/L	[32]
Exit Temperature	4°C	[15]
Centrifugation time	30min	[15]
Centrifugation P-8		
Sedimentation Efficiency	30%	Defined
Nucleic acid Removal	100%	Defined
Proteins Removal	5%	Defined
Solid Concentration in Heavy Stream	200 g/L	Defined
Exit Temperature	4°C	Defined
Centrifugation time	30min	[9]
Chromatograph P-9		
Resin Binding Capacity	29.40 g/L	Table 7.3.1

T7 RNAP binding	100%	Defined
T7 RNAP yield	89%	[13]
Resin Binding Capacity Utilization	70%	Defined
Loading & elution flowrate	3.5 BV/h	Table 7.3.2
Eluent Volume	4.00 BV	Defined
Elution gradient	50-500mM	[9]
Diafiltration P-14		
Volume Permeated	1	Defined
Contaminants Rejection Coefficients	0.00	Defined
T7 RNAP Rejection Coefficient	1.00	Defined
Product Denaturation	5%	Defined
Filtration time	240min	Defined

*For base case. Changed during sensitivity analysis.

7.2 Appendix 2 Yields

Four different scenarios for T7 RNAP yield has been considered and calculated into mass coefficients for a material balance, which is required input for cell disruption in the high-pressure homogenization. Firstly, one scenario has been built based on solely the composition of *E.coli*, see Table 7.2.1. Then, three scenarios have been made based on literature from Zawadzki *et al*, Davanloo *et al* and Milligan *et al* (presented in Table 3.2.2), see Table 7.2.2Table 7.2.4.

The T7 RNAP yields presented in Table 3.2.2, describes the amount of purified T7 RNAP, in other words the amount of T7 RNAP after all purification steps. A purification yield was identified for the model using following formula $\frac{\text{T7 RNAP amount in product stream}}{\text{T7 RNAP amount after homogenization}}$. By simulating the model based on process parameters in Table 7.1.2 and base case T7 RNAP yield 11.25mg/g *E.coli* as input for the homogenization, the purification yield 77% was identified. Consequently, the unpurified T7 RNAP output from the homogenization requires 11.25mg/g /0.77 = 14.61mg unpure T7 RNAP/g *E.coli* for the base case. Similar calculation adjustments were made for T7 yields originated from Davanloo *et al* and Milligan *et al*.

Table 7.2.1 E.coli composition adjusted according to section 3.2.2.1. Each component´s dry cell volume % were calculated by dividing its wet volume % by 30% (representing contents excl. water). Mass coefficients for material balance were based on 10 as mass coefficient for biomass, and it was assumed that volume % for dry cell can be converted to mass coefficient.

Component	**Volume %**	**Volume % (dry cell)**	**Mass coefficient**
Water	70.00	0	0
Nucleic Acids	7.00	23.3	2.33
T7 RNAP	1.70	5.7	0.57
Proteins excl. T7 RNAP	9.63	32.1	3.21
Cell debris	11.67	38.9	3.89

Table 7.2.2 Base case, based on T7 RNAP yield from Zawadzki et al. Each component´s dry cell volume % were calculated by dividing its wet volume % by 30% (representing contents excl. water). Mass coefficients for material balance were based on 10 as mass coefficient for biomass, and it was assumed that volume % for dry cell can be converted to mass coefficient.

Component	**Calculation for volume %**	**Volume %**	**Volume % (dry cell)**	**Mass coefficient**
Water	Fixed from composition, Table 3.2.1	70.00	0	0
Nucleic Acids	Fixed from composition, Table 3.2.1	7.00	23.33	2.33
T7 RNAP	$\frac{\text{amount of purified T7 RNAP [mg] per g } E.coli}{\text{purification yield}} = \frac{11.25}{0.77}$ =14.61 mg unpure T7 RNAP/g *E.coli* Assuming *E.coli* density as 1000 g/L	1.46	4.87	0.49
Proteins excl. T7 RNAP	$\frac{(T7\ RNAP\ volume\%)}{(T7\ RNAP\ part\ of\ total\ proteins)} - (T7\ RNAP\ volume\%) = \frac{1.46}{0.15} - 1.46$	8.28	27.60	2.76
Cell debris	100 minus the sum of above volume %	13.26	44.20	4.42

Table 7.2.3 Scenario based on T7 RNAP yield from Davanloo et al. Each component´s dry cell volume % were calculated by dividing its wet volume % by 30% (representing contents excl. water). Mass coefficients for material balance were based on 10 as mass coefficient for biomass, and it was assumed that volume % for dry cell can be converted to mass coefficient.

Component	**Calculation for volume %**	**Volume %**	**Volume % (dry cell)**	**Mass coefficient**
Water	Fixed from composition, Table 3.2.1	70.00	0	0
Nucleic Acids	Fixed from composition, Table 3.2.1	7.00	23.33	2.33
T7 RNAP	$\frac{\text{amount of purified T7 RNAP [mg] per g E. coli}}{\text{purification yield}} = \frac{15}{0.77}$ =19.48 mg unpure T7 RNAP/g *E.coli* Assuming *E.coli* density as 1000 g/L	1.95	6.49	0.65
Proteins excl. T7 RNAP	$\frac{(T7\ RNAP\ volume\%)}{(T7\ RNAP\ part\ of\ total\ proteins)} - (T7\ RNAP\ volume\%) = \frac{1.95}{0.15} - 1.95$	11.04	36.80	3.68
Cell debris	100 minus the sum of above volume %	10.01	33.38	3.34

Table 7.2.4 Scenario based on T7 RNAP yield from Milligan et al. Each component´s dry cell volume % were calculated by dividing its wet volume % by 30% (representing contents excl. water). Mass coefficients for material balance were based on 10 as mass coefficient for biomass, and it was assumed that volume % for dry cell can be converted to mass coefficient.

Component	**Calculation for volume %**	**Volume %**	**Volume % (dry cell)**	**Mass coefficient**
Water	Fixed from composition, Table 3.2.1	70.00	0	0
Nucleic Acids	Fixed from composition, Table 3.2.1	7.00	23.33	2.33
T7 RNAP	$\frac{\text{amount of purified T7 RNAP [mg] per L cell culture}}{\text{purification yield}} = \frac{30}{0.77}$ =38.96 mg unpure T7 RNAP/L cell culture Converted to 3.89 mg unpure T7 RNAP /g *E.coli* using biomass yield 10 g wet weight *E.coli*/L cell culture as Milligan *et al* refers to Davanloo *et al*. Assuming *E.coli* density as 1000 g/L.	0.39	1.30	0.13
Proteins excl. T7 RNAP	$\frac{(T7\ RNAP\ volume\%)}{(T7\ RNAP\ part\ of\ total\ proteins)} - (T7\ RNAP\ volume\%) = \frac{0.39}{0.15} - 0.39$	2.21	7.36	0.74
Cell debris	100 minus the sum of above volume %	20.40	68.01	6.80

7.3 Appendix 3 Calculations for Chromatograph

Table 7.3.1 Calculation of column volume for chromatograph.

	Value	**Source/calculation**
Binding capacity [mg/mL resin]	42	[37]
Part resin (vs void) of column	0.7	Defined
Binding capacity [mg/mL column]	**29.40**	=42*0.7
Utilization binding capacity	0.70	Defined
Concentration to load [mg/mL column]	20.58	=29.40*0.70
Amount T7 RNAP loaded [mg]	1050	SPD
Column volume [mL]	**51***	=1050/20.58

*51mL was approximated to a 50mL column due to adjusting for commercial availability.

Table 7.3.2 Flow velocity for elution and binding in chromatograph.

	Value	**Source/calculation**
Flowrate [mL/min]	3	[9]
Flowrate [mL/h]	180	=3*60
Column volume [mL]	51	Table 7.3.1
Input for SPD [BV/h]	3.5	180/51

7.4 Appendix 4 Cost data

Table 7.4.1 Costs of WFI, utilities, labour and time parameters.

Parameter	Value	Unit	Source
WFI	0.0205*	USD/kg	[60]
Utilities			
Cooling Water	0.0858	USD/ton	[61]
Chilled Water	0.0858	USD/ton	[61]
Electricity	2.1299**	USD/kWh	[62]
Glycol	0.8000	USD/MT	SPD default
Labour			
Basic rate	6.87	USD/h	[63]
Benefits factor	0.40		SPD default
Operating Supplies Factor	0.10		SPD default
Supervision Factor	0.20		SPD default
Administration Factor	0.60		SPD default
Adjusted rate	15.81		Calculated from above
Direct Time utilization	85	%	Defined
Time Parameters			
Year of Analysis and Construction	2022		Defined
Construction Period	30	Months	Defined
Startup Period	6	Months	Defined
Project Lifetime	25	Years	Defined
Inflation (to update equipment cost)	7.6	%	[64]
Other			
Income tax	25	%	SPD default
Depreciation period***	10	Years	SPD default
Laboratory (quality work)	15	% of total labour cost	SPD default
Startup & validation cost	5	% of DFC	SPD default
Working capital	30	Days****	SPD default

* An average cost of water purification process based on four different purification methods.
** Based on energy charge R2.294/kWh, service charge R80.45/day which was converted to kWh by assuming electricity usage of 213kWh and manufacturing time of total 1110h (resulted from base case during model development) as well as manufacturing capacity of 12h per day.
***Salvage fraction of 5% was assumed as SPD suggests. Performed using straight-line method.
****The working capital was estimated to cover expenses for 30 days of labour, raw materials and utilities.

Table 7.4.2: Exchange rates accessed September 2022 from https://www.xe.com/.

$	**ZAR**	**€**
1	17.48	0.999193

For capital investment the direct fixed capital (DFC) was estimated based on total equipment purchase cost, with distributed set of purchase cost factors. The factors are in three categories: direct cost, indirect cost and other cost which are summed up to obtain DFC. The factors set by SPD default was used, which can be seen in Table 7.4.3.

Table 7.4.3 Direct Cost, Indirect Cost and Other Cost factors based on total equipment Purchase cost, used in SPD to calculate Direct Fixed Capital. The values presented in the table are SPD default setting.

Direct Cost factors	
Piping	0.35
Instrumentation	0.40
Insulation	0.03
Electrical Facilities	0.10
Buildings	0.45
Yard Improvement	0.15
Auxiliary Facilities	0.40
Indirect Cost Factors	
Engineering	0.25
Construction	0.35
Other Cost Factors	
Constrictor's Fee	0.05
Contingency	0.10

7.5 Appendix 5 Microscale sensitivity analysis protocol

Three categories of changes were made in the model to determine how sensitive the model is to increase in biomass yield (upstream), changes in T7 RNAP yield (downstream) and the combination of changes in both upstream and downstream. This was done to represent effects from data yields reported in other references than Zawadzki *et al* which was used for the base case.

1) Upstream – Increased biomass yield, reference Davanloo *et al*
    a. Seed train
        i. Changed biomass yield to 3g/L in ferment operation unit for seed bioreactor
        ii. To be able to achieve this new concentration of *E.coli,* glucose concentration was increased to 6.1g/L, which achieved a glucose conversion of 98.44%. No other raw material volumes were changed.
        iii. To keep OD=0.1 (0.24g *E.coli*) in main bioreactor, the pull in volume from seed bioreactor was changed to 0.0824 L.
    b. Main bioreactor
        i. Kept changes from seed train above.
        ii. Changed biomass yield to 3g/L in ferment operation unit for main bioreactor
        iii. To be able to achieve this new concentration of *E.coli*, glucose concentration was increased to 7.9g/L, which achieved a glucose conversion of 94.92%. The input of ammonia also required to be increased to achieve the *E.coli* concentration. To keep 13% excess above stochiometric amount, volume was increased to 0.005L. No other raw material volumes were changed.
        iv. Material and energy balances were solved by SPD.
        v. Chromatograph column size was changed to 60ml based on the resulting T7 RNAP load (1280mg).
2) Downstream- Changes of T7 RNAP yield in homogenization
    a. Milligan *et al* – lower yield
        i. Change mass coefficients for the material balance in the homogenization (P-4), according to Table 7.2.4.
        ii. Material and energy balances were solved by SPD.
        iii. Chromatograph column size was changed to 15ml based on the resulting T7 RNAP load (260mg).
    b. Composition *et al* – slight higher yield
        i. Change mass coefficients for the material balance in the homogenization (P-4), according to Table 7.2.1.
        ii. Material and energy balances were solved by SPD.
        iii. Chromatograph column size was changed to 60ml based on the resulting T7 RNAP load (1230mg).
    c. Davanloo *et al*– much higher yield
        i. Change mass coefficients for the material balance in the homogenization (P-4), according to Table 7.2.3.
        ii. Material and energy balances were solved by SPD.
        iii. Chromatograph column size was changed to 70ml based on the resulting T7 RNAP load (1420mg).

3) Combination – both upstream and downstream changes
    a. Davanloo *et al* reference for biomass yield and purified T7 RNAP yield.
        i. Followed procedure 1a,b and 2c above, except the column size.
        ii. Material and energy balances were solved by SPD.
        iii. Chromatograph column size was changed to 85ml based on the resulting T7 RNAP load (1750mg).
    b. Milligan *et al* reference for biomass yield and purified T7 RNAP yield.
        i. Followed procedure 1a,b and 2a above, except the column size. Material and energy balances were solved by SPD.
        ii. Chromatograph column size was changed to 15ml based on the resulting T7 RNAP load (320mg).

Note, loading and eluate flowrate of the chromatograph was not adjusted even though the column volume was adjusted. Since the flowrate was expressed in bed volumes per hour, the new column volume was already automatically included. It could be argued that the flowrate should be changed based on calculations in Table 7.3.2. However, those calculations requiring the column volume, were based on the flowrate 3mL/min which originates from a source with a column volume close to the base case. Hence, when scaling the column volume this flowrate can be considered as inadequate.

7.6 Appendix 6 Raw materials process summary

Table 7.6.1 Materials cost - process summary of base case.

Bulk Material	**Unit Cost [$]**	**Annual Amount [kg]**	**Annual Cost [$]**	**%**
β-mercaptoethanol	36.27	0	1	0.02
Air	0.00	13	0	0.00
Ammonia	24.20	7	169	4.66
Dipotassium phosphate	25.62	0	0	0.01
DTT	46.27	0	0	0.00
EDTA Disodium	27.69	0	1	0.03
Glucose	24.71	3	70	1.92
Glycerol	24.64	8	199	5.48
IPTG	885.18	2	1,449	39.85
Kanamycin sulphate	69.23	0	3	0.09
Sodium chloride	23.84	0	5	0.13
Streptomycin sulphate	839.00	2	1,720	47.30
TRIS-HCl	86.27	0	9	0.23
WFI	0.02	494	10	0.28
TOTAL			3,636	100.00

7.7 Appendix 7 Results microscale sensitivity analysis

Table 7.7.1 Parameters and results of microscale sensitivity analysis.

Scenario	**Base case**	**A**	**B**	**C**	**D**	**E**	**F**	**G**
File number in SPD	-	8	9	4	5	6	7	10
Change from base case	-	Downstream: 73% lower T7 RNAP yield	Downstream: 14% higher T7 RNAP yield	Downstream: 33% higher T7 RNAP yield	Upstream seed bioreactor: 25% higher biomass yield	Upstream both bioreactors: 25% higher biomass yield	Combination Up- & Downstream	Combination Up- & Downstream
Reference for change	-	Milligan *et a*l, Table 7.2.4	Composition based, Table 7.2.1	Davanloo *et al*, Table 7.2.3	Davanloo *et al,* Table 3.2.2	Davanloo *et al*, Table 3.2.2	Davanloo *et al*, Table 3.2.2 & Table 7.2.3	Milligan *et al*,Table 3.2.2 & Table 7.2.4
T7 yield mass coeff.	0.49	0.13	0.57	0.65	0.49	0.49	0.65	0.13
Biomass yield* Seed bioreactor [g *E.coli*/L]	2.4	2.4	2.4	2.4	3.0	3.0	3.0	3.0
Biomass yield* Main bioreactor [g *E.coli*/L]	2.4	2.4	2.4	2.4	2.4	3.0	3.0	3.0
Results below								
Throughput [g/year]	38.3	9.4	45	52	38.2	46.8	63.7	11.4
Recovery T7 yield [g]	78%	72%	79%	79%	78%	76%	78%	70%
T7 RNAP cost [$/kg T7 RNAP]	62 689 593	258 419 437	53 204 980	46 056 499	62 802 918	51 251 281	37 500 935	213 496 112
Cost reduction		-312.2%	15.1%	26.5%	-0.2%	18.2%	40.2%	-240.6%
AOC [$]	2 399 000	2 426 000	2 396 000	2 393 000	2 399 000	2 396 000	2 388 000	2 427 000
Total capital investment [$]	12 786 000	12 902 000	12 771 000	12 756 000	12 786 000	12 772 000	12 734 000	12 903 000
Gross Margin	54%	-90%	61%	66%	54%	62%	72%	-57%
ROI	25.5%	0.1%	31.0%	36.6%	25.5%	32.3%	46.1%	2.2%
Payback time [years]	3.92	1029.11	3.23	2.74	3.93	3.09	2.17	45.85
IRR	21.33%	N/A	25.27%	28.99%	21.30%	26.22%	34.91%	N/A
NPV [$]	19 250 000	-11 244 000	25 952 000	32 812 000	19 182 000	27 651 000	44 439 000	-8 884 000

* Dry Biomass yield. Wet biomass yield from Table 3.2.2 converted to dry by multiplying with 0.3 (70% of *E.coli* is composed of water according to Table 3.2.1).